Earth-Science Reviews 141 (2015) 82–104

Contents lists available at ScienceDirect

Earth-Science Reviews

journal homepage: www.elsevier.com/locate/earscirev

A review of deformation pattern templates in foreland basin systems and fold-and-thrust belts: Implications for the state of stress in the frontal regions of thrust wedges

S. Tavani [a,*], F. Storti [b], O. Lacombe [c,d], A. Corradetti [a], J.A. Muñoz [e], S. Mazzoli [a]

[a] Dipartimento di Scienze della Terra, dell'Ambiente e delle Risorse, Università Federico II, Napoli, Italy
[b] NEXT — Natural and Experimental Tectonics Research Group, Dipartimento di Fisica e Scienze della Terra "Macedonio Melloni", Università di Parma, Italy
[c] Sorbonne Universités, UPMC Univ. Paris 06, UMR 7193, ISTeP, Paris, France
[d] CNRS, UMR 7193, ISTEP, F-75005, Paris, France
[e] Geomodels, Departament de Geodinàmica i Geofísica, Facultat de Geologia, Universitat de Barcelona, Spain

ARTICLE INFO

Article history:
Received 16 July 2014
Accepted 25 November 2014
Available online 2 December 2014

Keywords:
Thrust and fold belt
Fractures
Stress
Anticlines
Inversion tectonics
Foreland

ABSTRACT

Aesthetically appealing thrust systems and related large-scale anticlines, in both active and fossil foreland fold-and-thrust belts, and the economic potential associated with them, have captured the interest of structural geologists for many decades. As a consequence, a large amount of data on sub-seismic deformation patterns from thrust-related anticlines is available in the literature. We provide a review of deformation pattern templates from field data in foreland fold-and-thrust-belts and show that the most frequent trends of sub-seismic syn-orogenic deformation structures hosted in km-scale thrust-related folds frequently and paradoxically indicate a syn-thrusting strike-slip stress field configuration, with a near-vertical σ_2 and a sub-horizontal σ_3, rather than a contractional one where the latter is expected to be the vertical principal axis of the stress ellipsoid. This apparent inconsistency between sub-seismic syn-orogenic deformation structures and stress field orientation is here named "the σ_2 paradox". Field data support a possible explanation of the paradox, provided by the major role played by inherited early-orogenic extensional deformation structures on thrust fault nucleation. Nucleation of major thrusts and their propagation is facilitated and driven by the positive inversion and linkage of the early-orogenic sub-seismic extensional inheritance developed in the foreland basin. This process eventually leads to the development of large reverse fault zones and can occur both in contractional and strike-slip stress field configurations.

Contents

* Corresponding author at: Stefano Tavani Dipartimento di Scienze della Terra, dell'Ambiente e delle Risorse Università degli Studi di Napoli Federico II Largo San Marcellino 10, 80138 Napoli, Italy. Tel.: + 39 081 2538155; fax: + 39 0812538338.
E-mail address: stefano.tavani@unina.it (S. Tavani).

http://dx.doi.org/10.1016/j.earscirev.2014.11.013
0012-8252/

1. Introduction

Many of the most prolific hydrocarbon systems in the world are hosted in foreland fold-and-thrust belts, where oil migration and accumulation are controlled by deformation structure networks. The use of deformation pattern templates for supporting predictions in reservoirs has significantly contributed to an impressive number of structural studies in foreland fold-and-thrust belts and in the adjacent foreland basin systems (DeCelles and Giles, 1996) since the late 60s (Stearns, 1968; Stearns and Friedman, 1972; McQuillan, 1974; Engelder and Geiser, 1980; Geiser and Sansone, 1981; Hancock, 1985; Marshak and Engelder, 1985; Price and Cosgrove, 1990; Srivastava and Engelder, 1990; Gray and Mitra, 1993; Mitra et al., 1984; Protzman and Mitra, 1990; Ferrill and Groshong, 1993; Lemiszki et al., 1994; Holl and Anastasio, 1995; Railsback and Andrews, 1995; Thorbjornsen and Dunne, 1997; Fischer and Jackson, 1999; Lacombe et al., 1999; Storti and Salvini, 2001; Silliphant et al., 2002; Graham et al., 2003; Sans et al., 2003; Bellahsen et al., 2006a; Wennberg et al., 2006; Lacombe et al., 2006, 2011; Tavani et al., 2006a; Lash and Engelder, 2007; Stephenson et al., 2007; Ahmadhadi et al., 2007, 2008; Amrouch et al., 2010a; Evans, 2010; Savage et al., 2010; Casini et al., 2011; Shackleton et al., 2011; Tavani et al., 2011a, 2011b; Beaudoin et al., 2012; Keating et al., 2012; Tavani et al., 2012a; Awdal et al., 2013; Carminati et al., 2013, among others). A common observation in the great majority of this kind of study is the occurrence, in cylindrical folds, of a deformation pattern characterised by (i) contractional and extensional deformation structures trending parallel to the fold axis (longitudinal structures), (ii) extensional deformation structures trending perpendicular to the fold axis direction, and (iii) conjugate strike-slip faults trending at high angle to the fold axis direction (e.g. Hancock, 1985; Cooper, 1992). The latter two are defined as transversal structures (e.g. Storti and Salvini, 1996) (Fig. 1).

The Andersonian theory of faulting (Anderson, 1951) predicts for orogenic systems a contractional stress ellipsoid with a vertical minimum principal axis σ_3. This assumption has enjoyed widespread adoption in analytical (e.g. Elliott, 1976; Chapple, 1978; Davis et al., 1983; Dahlen et al., 1984; Fletcher, 1989) and numerical models (e.g. Koons, 1995; Beaumont et al., 1996; Simpson, 2011; Ruh et al., 2012) of thrust wedge dynamics and kinematics. Field-based structural geology and deformation microstructure analysis (e.g. calcite twins, Lacombe, 2010), document that the principal axis σ_3 has been mostly sub-horizontal over large areas, both before and during thrusting (e.g. Lacombe et al., 2012). This observation that σ_3 rather than σ_2 is horizontal in fold and thrust belts, implies stresses associated with strike-slip rather than compression, and is referred to here as the σ_2 paradox. In the following sections, we provide a review of the typical structural assemblages that occur in the different sectors of foreland fold-and-thrust belts and foreland basin systems, with the twofold purpose of: (1) discussing how inherited extensional structures developed during foreland flexure/foredeep formation can provide properly oriented discontinuities facilitating the nucleation of large thrusts, even when σ_3 instead of σ_2 lies on fault surfaces; (2) placing constraints on the stress field evolution before and during thrusting, showing and discussing a robust explanation of the σ_2 paradox. Available data, in fact, suggest for two early-orogenic extensional stress field configurations characterised by mutually perpendicular layer-parallel stretching directions, respectively (Fig. 2). This deformation predates layer parallel shortening (LPS), which very frequently occurs in a strike-slip stress field configuration. Subsequent thrusting and fold amplification may imply a severe time-space dependent reorganisation of the stress field that, in the majority of the structural positions within folds, can continue to be characterised by a sub-horizontal σ_3.

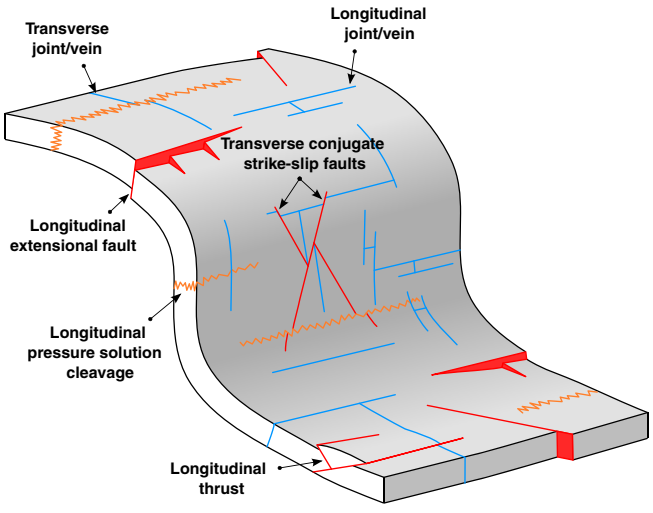

Fig. 1. Geometry of deformation structures commonly observed in thrust-related anticlines.

2. Deformation structure patterns in foreland fold-and-thrust belts

Despite its apparent simplicity (Fig. 1), the deformation pattern recorded in fold-and-thrust-belts typically results from a long-lasting pathway that can be schematically simplified in six major stages (Fig. 2): (i) foreland flexuring, taking place in the peripheral bulge and in the outermost region of the foredeep; (ii) along-strike stretching, occurring in the foredeep; (iii) layer-parallel shortening, which may occur both in the innermost region of the foredeep and at the toe of thrust wedges; (iv) syn-folding deformation sensu-stricto, occurring during the growth of thrust-related anticlines; (v) late stage fold tightening; and (vi) gravity-driven extensional deformation.

2.1. Foreland-flexuring

Convergent plate margins are characterised by the development of extensional deformation structures such as joints, veins and dilation bands, oriented parallel to the belt-foreland basin system (Fig. 3A). These structures, which form the older syn-orogenic assemblage, are associated with the flexure of the downgoing lithosphere. Flexuring causes outer-arc extension in the peripheral bulge and in the outermost sector of the foredeep (Turcotte and Schubert, 1982; Bradley and Kidd, 1991; Doglioni, 1995; Langhi et al., 2011). The minimum principal axis of the stress ellipsoid σ_3 lies on the bedding surfaces and strikes perpendicular to the foredeep trend. The effective minimum principal axis of the stress ellipsoid can attain negative values in the shallow subsurface, whilst the effective minimum stress can attain negative values also at depth. Development of longitudinal extensional faults with rather constant, high cutoff angles during this stage, indicates that the overburden favours a stress field with a positive and sub-vertical σ_1. Perpendicularity between bedding and σ_1 in the entire peripheral bulge area ensures that slip along bedding-parallel anisotropies is inhibited. The σ_2 principal axis of the stress ellipsoid strikes orthogonal to the σ_1–σ_3 plane, that is sub-horizontal and parallel to the peripheral bulge trend. Foreland flexure-related deformation structures are increasingly documented in both exposed foreland areas and within the adjacent fold-and-thrust belt frontal regions (Calamita and Deiana,

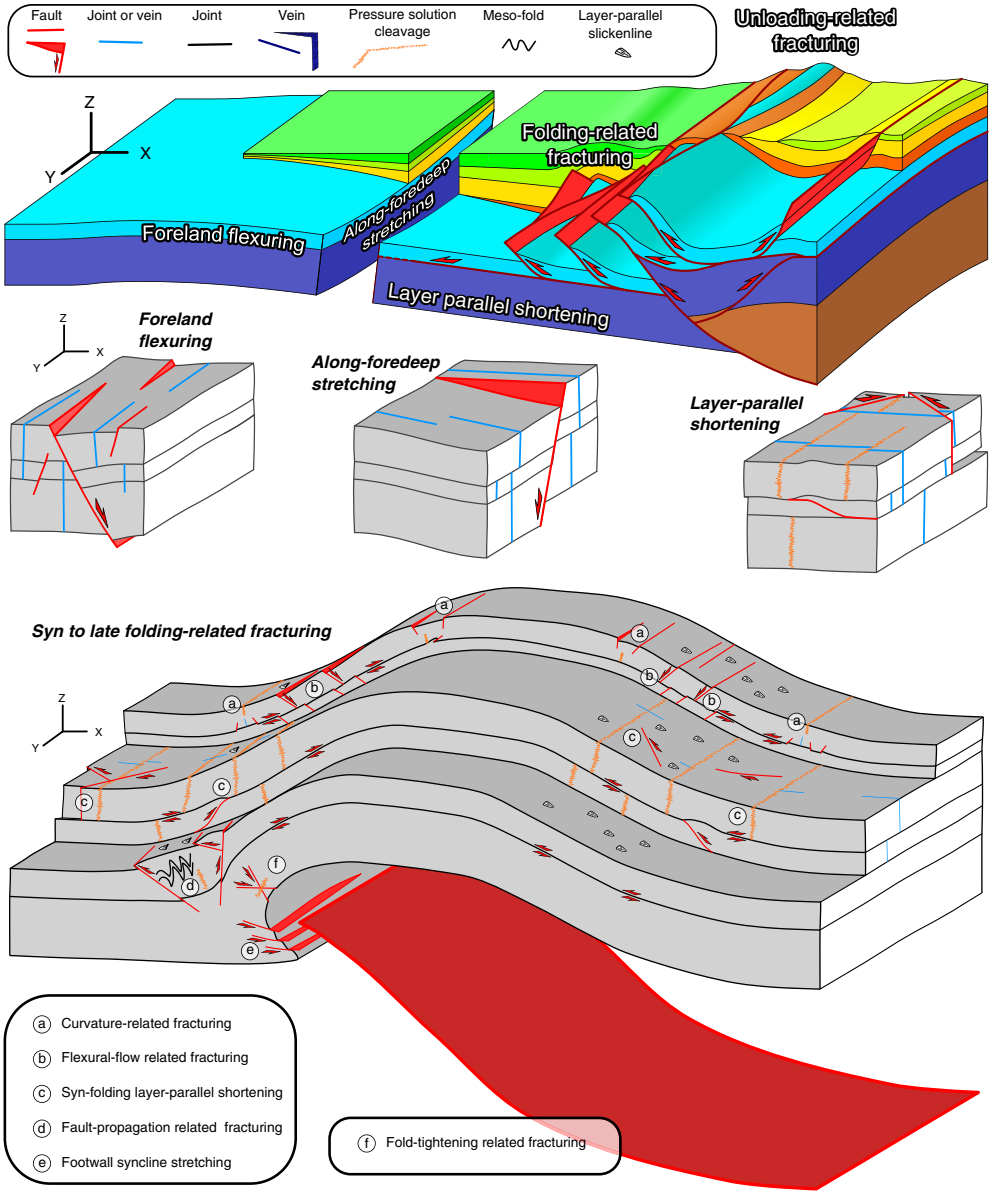

Fig. 2. 3D scheme showing the architecture of a foreland fold-and-thrust belt and the typical structural assemblages developing during the five syn-orogenic deformation stages described in this work.

1980; Scisciani et al., 2001; Billi and Salvini, 2003; Mazzoli et al., 2005; Lash and Engelder, 2007; Casini et al., 2011; Beaudoin et al., 2012; Quintà and Tavani, 2012; Tavani et al., 2012a). Foreland flexure-related extensional faults are frequently imaged in seismic cross-sections across foreland areas (Fig. 3B) (e.g. Lorenzo et al., 1998; Matenco and Bertotti, 2000; Ranero et al., 2003). During this early deformation stage, longitudinal jointing, veining, and extensional faulting may occur at different locations, depending on factors including syn-orogenic sediment thickness, as well as curvature and elastic thickness of the lithosphere. Jointing is expected in the maximum curvature area and at the shallower structural levels, as there the fibre-stress can allow for negative values of σ_3 (stage 1.1 in Fig. 3A). The presence of fluids can widen the lateral and vertical extent of the area where the effective minimum stress equals the tensile strength of the intact rock (stage 1.2 in Fig. 3A). As the thickness of syn-orogenic sediments increases towards the belt, the maximum principal axis of the stress ellipsoid σ_1 increases as well, favouring extensional faulting in a hinterlandward position with respect to the maximum curvature area (stage 1.3 in Fig. 3A). Transversal extensional deformation structures, oriented perpendicular to the longitudinal ones, can also form during flexuring (e.g. Destro, 1995; Quintà and Tavani, 2012). They include cross-joints (e.g. Gross, 1993) associated with stress release (requiring negative values of σ_2; Bai et al., 2002), and release faults accommodating hanging wall fault-parallel stretching induced by the lateral decrease of fault displacement (Destro, 1995; Medwedeff and Krantz, 2002) (Fig. 4). Joints, veins, and dilation bands developed during foreland flexuring are oriented perpendicular to bedding, whilst extensional faults have constant cutoff angles. Diagnostic features of these deformation structures, allowing one to recognise them when the hosting layers are incorporated into fold-and-thrust belts, include: (1) constant strike over large areas, since these structures respond to a lithospheric scale process; (2) the preservation of their angular relationships with bedding at different bedding dip values; (3) the crosscutting/abutting relationships with respect to shortening-related structures; (4) the lack, within the same mechanical unit, of significant frequency variability in the different structural positions across thrust-related folds. The last point is particularly important, since: (i) foreland flexuring-related deformation structures may undergo syn-folding reactivation, which

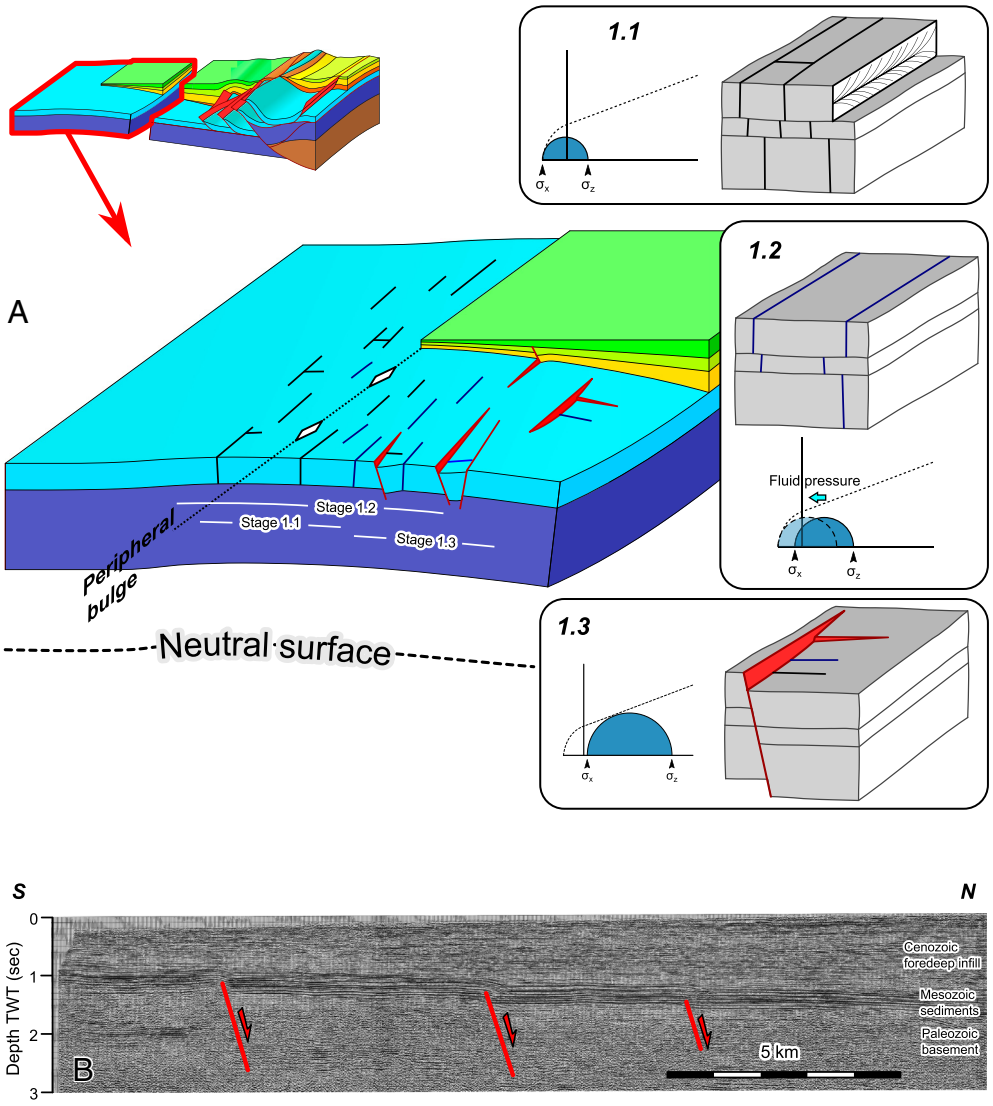

Fig. 3. A) Foreland flexuring extensional deformation stage associated with outer arc extension in the peripheral bulge. This process leads to the development of longitudinal (i.e. oriented parallel to the forebulge–foredeep–belt system) extensional structures that, according to their type, can occur at different locations and depths. Possibly, transverse structures can develop as secondary features. B) Seismic section across the Duero Foreland Basin (Northern Spain), striking perpendicular to the trend of the foredeep and showing foreland flexuring related longitudinal extensional faults.

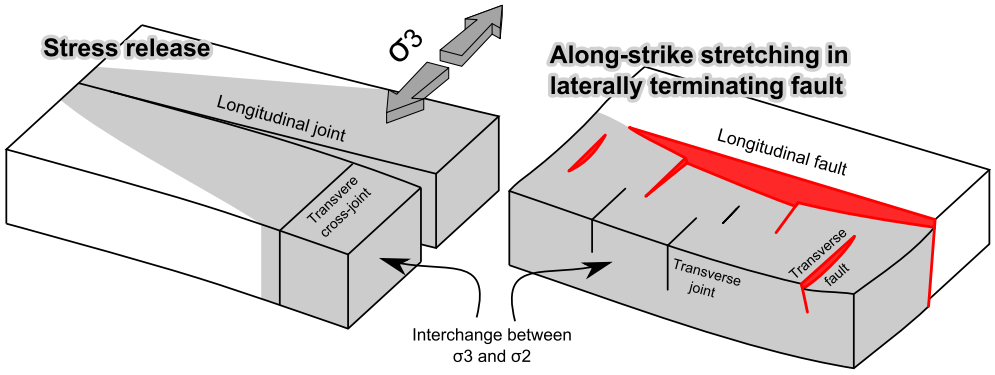

Fig. 4. Deformation mechanisms allowing the development of transverse extensional structures. On the left, the stress release mechanism (Bai et al., 2002), where an opening longitudinal joint acts as a traction-free surface. Along the joints the magnitude of the stress component paralleling the regional stretching direction becomes zero and an area of stress reduction surrounds the joint. There, provided the regional σ_2 is negative, a permutation between the regional σ_3 and σ_2 can occur, with the consequent development of transverse joints. The along strike stretching mechanism (Destro, 1995) is illustrated on the right. There, during faulting the laterally decreasing displacement along the fault causes fault-parallel lengthening in the hanging-wall. Such lengthening imposes a local extensional stress oriented perpendicular to the regional σ_3. Possibly, the same mechanism can operate in the foot-wall undergoing differential uplift.

modifies their original croscutting relationships; (ii) similar deformation structures having the same trend and the same constant angular relationships with bedding may develop during thrusting and folding, but only in some specific sectors of the folds.

2.2. Along-foredeep stretching

Progressive underthrusting of the lower plate lithosphere causes rock migration from the foreland flexured zone into the monoclinal-dipping area of the foredeep. Lateral variability and terminations of orogenic systems impose along-strike curved profiles to foredeeps (Fig. 5), which are attained by along-strike stretching. When the across strike curvature is negligible, this process can cause σ_3 to become oriented almost parallel to both bedding and foredeep trend (Quintà and Tavani, 2012). The amount of foredeep parallel stretching increases with increasing subsidence in the central region and, in many cases, σ_3 can become negative. At this stage, the sedimentary overburden still provides the maximum acting stress and, consequently, σ_2 is oriented perpendicular to the trend of the foredeep. In essence, the transition from foreland flexure to the along-strike stretched foredeep implies interchange of σ_2 and σ_3, as the peripheral bulge and the foredeep axial trend are parallel. In many cases, where foreland flexuring has implied weak deformation, transverse extensional structures can represent the first syn-orogenic assemblage. This has been described for example in the Brunei deepwater fold and thrust belt (Morley et al., 2014), where polygonal faults developed in an isotropic stress field grade into transverse extensional faults approaching the fold and thrust belt (Fig. 6A). During along strike-stretching, joints are expected to develop in the upper portion of the sedimentary pile (Figs. 4, 6B, C), whilst with increasing depth and degree of diagenesis, the tensile strength can be overcame only in the case of fluid-assisted deformation. In such environmental conditions, σ_3 attains positive values and the vertical stress (σ_1) increases, thus favouring shear failure. The amount of along-strike foredeep stretching can increase in the case of curved orogens (e.g. Doglioni, 1995; Zhao and Jacobi, 1997; Whitaker and Engelder, 2006), because in this case it derives from the sum of cross-sectional and longitudinal curvature.

2.3. Layer parallel shortening (LPS)

Approaching the fold-and-thrust belt toe, the magnitude of the sub-horizontal component of the stress field, oriented parallel to the tectonic transport direction, increases until it exceeds the magnitude of the sub-vertical component. This is documented by finite strain data (e.g. Holl and Anastasio, 1995; Sans et al., 2003), and by the simple observation that the occurrence of contractional deformation structures increases towards the thrust wedge toe (e.g. Geiser and Engelder, 1983; Mitra et al., 1984). The site where the sub-horizontal principal axis of the stress ellipsoid oriented parallel to the tectonic transport direction becomes the maximum stress component, i.e. where the σ_1–σ_2 switching occurs, defines the external boundary of the layer-parallel shortening (LPS) domain (Fig. 7A). This boundary roughly coincides with the process zone of the sole thrust, as layer parallel shortening is, in essence, the mechanism by which the hanging wall accommodates the forelandward cross-sectional decrease of displacement, whilst the footwall does not deform (Fig. 7B) (e.g. Engelder and Engelder, 1977; Cooper et al., 1983; Williams and Chapman, 1983; Geiser, 1988; Evans and Dunne, 1991; Lacombe and Mouthereau, 1999; Koyi et al., 2004). LPS has been firstly described in North America (Nickelsen, 1966; Crosby, 1969; Engelder and Engelder, 1977; Allmendinger, 1982) and it is widely recognised in almost all the fold-and-thrust belts of the world, including the Appalachians (Engelder and Engelder, 1977; Geiser and Engelder, 1983; Wiltschko et al., 1985; Evans and Dunne, 1991), the Apennines (e.g. Alvarez et al., 1978; Geiser, 1988; Tavarnelli, 1997), the Norwegian Caledonides (Morley, 1986a), the Pyrenean Orogen (e.g. Averbuch et al., 1992; Rocher et al., 2000; Koyi et al., 2004; Tavani et al., 2006a; Quintà and Tavani, 2012), the Sevier fold-and-thrust belt (e.g. Weil and Yonkee, 2012), the Laramide belt (Amrouch et al., 2010a; Beaudoin et al., 2012), the Zagros (Lacombe et al., 2006, 2011; Ahmadhadi et al., 2008; Casini et al., 2011; Tavani

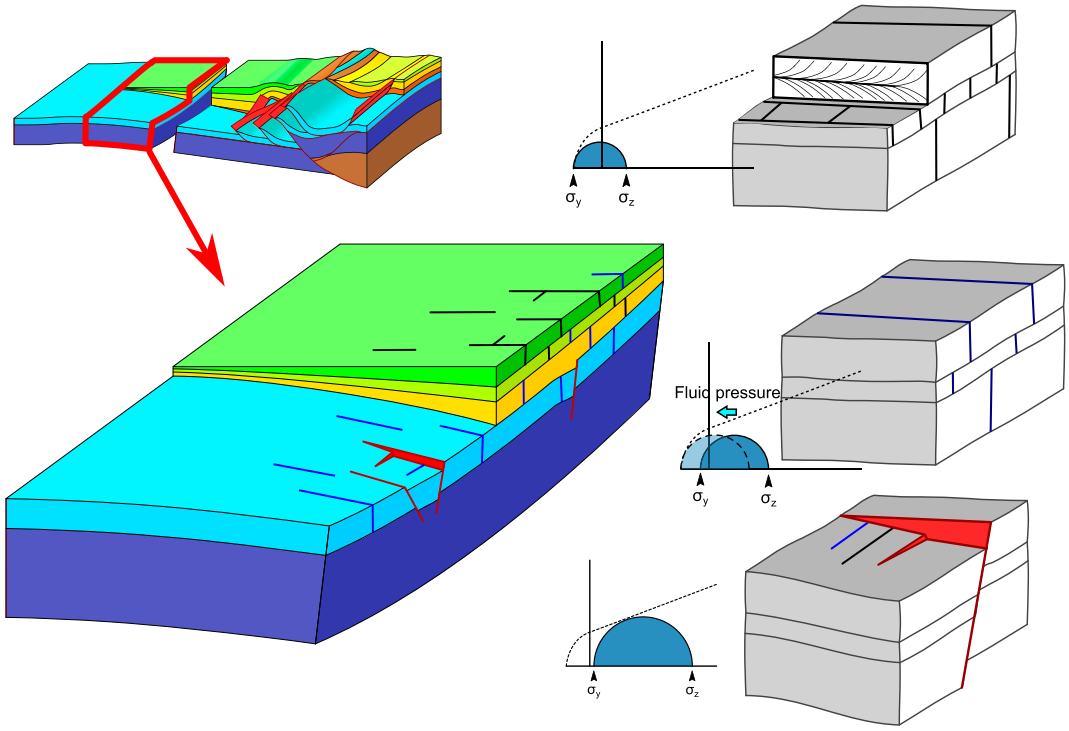

Fig. 5. Along-foredeep stretching deformation stage. It occurs because of a foredeep-parallel lengthening induced by cross-sectional concave shape acquisition of the foredeep. This process can lead to the development of transverse (i.e. striking perpendicular to the forebulge-foredeep-belt system) extensional structures that, according to their type, can occur at different locations and depths. Possibly, longitudinal structures can develop as secondary features.

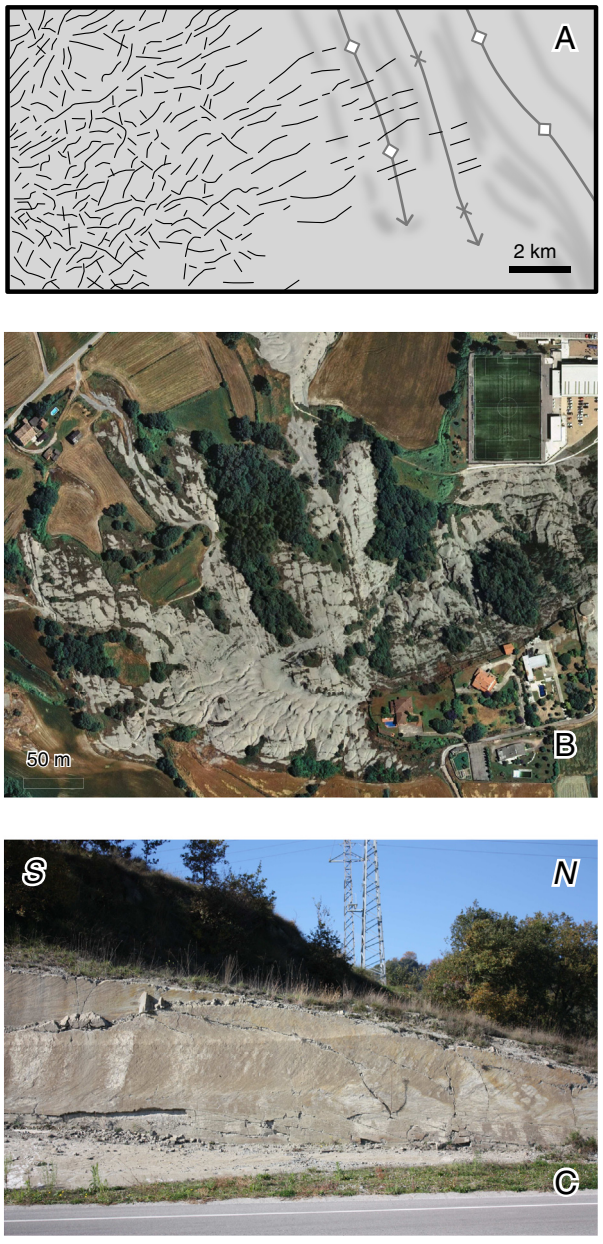

Fig. 6. A) Line-drawing of an original coerency time-slice in Morley et al. (2014), showing the frontal portion of a sector of the Brunei deepwater fold and thrust belt, with black lineations indicating transverse extensional faults within and immediately ahead (to the west) of the frontal anticline, progressively grading into polygonal faults n the foreland areas. B) Orthophoto (INSTITUTO GEOGRÁFICO NACIONAL DE ESPAÑA) from the Ebro Foreland Basin flanking to the south the E–W striking Pyrenean Orogen. The Orthophoto shows the trace of NNW–SSE striking transverse structures near the town of Vic. C) Photo from the same area, showing that these structures correspond to tens-metres long joints having well-recognisable plumose structures.

et al., 2011b), the Himalaya (e.g. Long et al., 2011), the Andes (e.g. Gonzales and Aydin, 2008; Torres Carbonell et al., 2013), the Anti-Atlas (e.g. Ismat, 2008), the Variscan orogen of northern Europe (e.g. Morley, 1986b; Nenna and Aydin, 2011), Taiwan (e.g. Lacombe et al., 1999, 2003; Chu et al., 2013), and the outer Carpathians (e.g. Mastella and Konon, 2002).

In sedimentary sequences, layer parallel shortening, formerly defined also as "lateral compaction" (e.g. Nickelsen, 1966), is accommodated by means of different deformation mechanisms in different materials and triggers development of deformation structures at both the meso- and micro-scale, so that it is recorded also by AMS in clay-rich sediments (e.g. Roure et al., 2005; Aubourg et al., 2010; Robion et al., 2012). For example, poorly consolidated granular sediments in the shallower structural levels of foreland fold-and-thrust belts may undergo micro-fracturing and pore-collapse accommodating compaction and volume loss (Fig. 7C) (Mollema and Antonellini, 1996), leading to preferred grain orientation (e.g., Amrouch et al., 2010b). Similarly, development of pressure solution cleavage in limestones may involve an initial pure compaction framework, which is achieved by synchronous calcite removal along stylolites and precipitation in the neighbouring pores (Fig. 7C) (e.g. Renard et al., 1997; Amrouch et al., 2010b). At this stage, shortening mainly occurs at the expense of porosity, and cases where up to 60-75% of the horizontal shortening is accommodated by consolidation and porosity loss are documented (e.g. Moore et al., 2011). When pore space reduction becomes less effective, further shortening requires bi- or triaxial strain. In limestone, pressure solution can continue to operate only if a significant volume of unsaturated water can circulate within the system (e.g. Engelder and Marshak, 1985), and/or calcite is precipitated in newly created spaces, which are typically provided by fractures oriented at about 90° from the pressure solution cleavage surfaces (Fig. 7D) (Fletcher and Pollard, 1981). The latter case results in a cleavage-perpendicular elongation. Consequently, pressure solution cleavage–vein pairs can be regarded as equivalents of conjugate fault systems, as both imply shortening along one direction and elongation perpendicular to it. In lithologies where dissolution is effective, pressure solution cleavage–vein systems can accommodate relatively large strain values (e.g. De Paor et al., 1991). The amount of shortening associated with them is typically higher than 5%–10% (e.g. Engelder and Engelder, 1977; Alvarez et al., 1978; Hudleston and Holst, 1984; Ferrill and Dunne, 1989; Protzman and Mitra, 1990; Holl and Anastasio, 1995; Evans et al., 2003). Pressure-solution cleavage–vein pairs oriented at a high angle to bedding are widely documented in carbonate rocks exposed both in foreland areas (Railsback and Andrews, 1995) and adjacent fold-and-thrust belts (e.g. Engelder and Geiser, 1980; Mitra and Adolph Yonkee, 1985; Tavarnelli, 1997; Evans and Elmore, 2006; Casini et al., 2011; Tavani et al., 2012b; Weil and Yonkee, 2012). When rocks are less prone to dissolution, stylolite-vein pairs are replaced by conjugate strike-slip faults at a high angle to bedding (Fig. 7E) (e.g. Stearns, 1968; Crosby, 1969; Marshak et al., 1982; Hancock, 1985; Price and Cosgrove, 1990; Cooper, 1992; Erslev and Rogers, 1993; Erslev, 2001; De Paola et al., 2006; Lacombe et al., 2006; Tavani et al., 2006a; Ismat, 2008; Amrouch et al., 2010a; Weil and Yonkee, 2012). The geometry of both strike-slip faults and pressure-solution cleavage-vein assemblages indicates a near bedding-perpendicular σ_2 and this means that shortening along the tectonic transport direction is accompanied by elongation along the strike of the thrust belt-foreland basin system. The expected "compressive Andersonian stress scenario" would have implied bedding-parallel veins that, however, are rarely documented in foreland fold-and-thrust belts (e.g. Séjourné et al., 2005). More abundant are subsidiary folds and thrusts accommodating bedding perpendicular elongation (Fig. 7F) (e.g. Lacombe et al., 1999; Weil and Yonkee, 2012).

Crucial for addressing the σ_2 paradox is the assessment of the relative abundance of meso-scale reverse faults versus strike-slip faults, pressure-solution cleavages and veins. This under the assumption that strain accommodated by each type of structure has the same order of magnitude. The datasets that we collected in thrust-related anticlines of many fold-and-thrust belts provide the relative abundance of meso-scale deformation structures within the same mechanical units, over representative large areas and show that reverse faults in carbonate rocks represent less than ~7% of the total LPS pattern; ~10% is represented by strike-slip faults, whilst pressure solution cleavage (computed only when in association with bedding perpendicular joints/veins) constitutes more than ~80% (Tavani et al., 2006a, 2008, 2011a, 2011b, 2012a, 2012b) (Fig. 8). It follows that deformation structures indicating bedding perpendicular σ_2 are about 15 times more abundant than those associated with bedding parallel σ_2. Such a value is expected to be

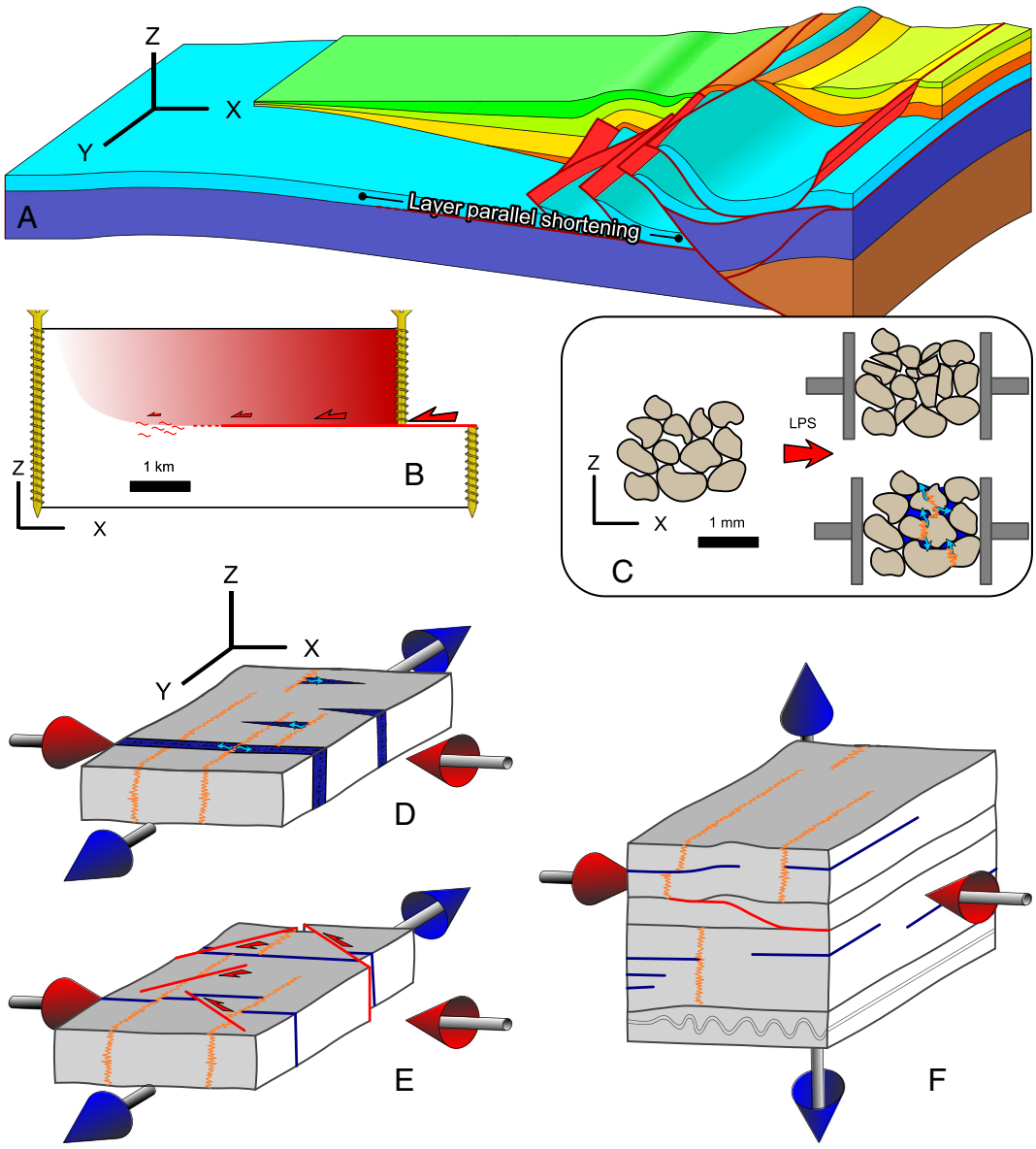

Fig. 7. Layer parallel shortening (LPS) stage. (A) Cross-sectional sector of the foreland fold-and-thrust belt where LPS occurs. (B) Scheme showing how the layer-parallel shortening essentially occurs to accommodate forelanward decreasing displacement along a layer-parallel decollement. (C) Micro-scale mechanisms accommodating LPS in granular materials during the first stages of LPS, both implying volume and porosity reduction. Meso-scale deformation patterns developed during LPS, implying either layer-parallel (D, E) or layer-perpendicular (F) elongation.

significantly lower in non-carbonate layers, where the occurrence of pressure solution cleavage is negligible. Amrouch et al. (2011) pointed out that during layer-parallel shortening in the Sheep Mountain Anticline (Wyoming, U.S.A.), the σ_2 principal axis of the stress ellipsoid was oriented near vertical, whilst it attained a sub-horizontal orientation during incipient folding and coeval development of reverse faults only close to the upward propagating thrust. Although opposite cases are documented (e.g. Averbuch et al., 1992; Fischer and Christensen, 2004; Neely and Erslev, 2009), the conclusion that reverse faults are generally a minor component of the LPS pattern, is supported by many published data. As an example, data in Crosby (1969) include only pressure-solution cleavage, veins and strike-slip faults. In the milestone paper of Geiser and Engelder (1983), pressure-solution cleavage and veins are abundantly described, whilst there is no mention of reverse faults. Evans and Elmore (2006) describe the LPS pattern by means of mutually orthogonal, bedding perpendicular pressure solution cleavages and veins. Finally, Chu et al. (2013) report that strike-slip faults are more abundant than thrust faults in Taiwan.

2.4. Folding-related deformation

Development and progressive modification of thrust-related folds determines the onset of up to six additional folding mechanisms that locally modify the regional stress field (Fig. 2): (a) bending-related tangential longitudinal strain, (b) flexural-slip, (c) syn-folding LPS, (d) deformation ahead of the upward propagating fault tip, (e) footwall syncline stretching, (f) gravity-driven extensional deformation.

2.4.1. Bending- and flexural slip-related deformation

Bending-related tangential longitudinal strain (e.g. Ramsay, 1967; Twiss and Moores, 1992; Lisle, 1994; Bobillo-Ares et al., 2000; Fischer and Wilkerson, 2000) is probably the most widely applied folding mechanism to explain deformation patterns in exposed thrust-related anticlines, and to make predictions in folds from reflection seismic data. The sedimentary pile is assumed to behave as a bending beam (hereinafter named the mechanical layer) undergoing tangential longitudinal strain. A neutral surface divides two areas undergoing layer-

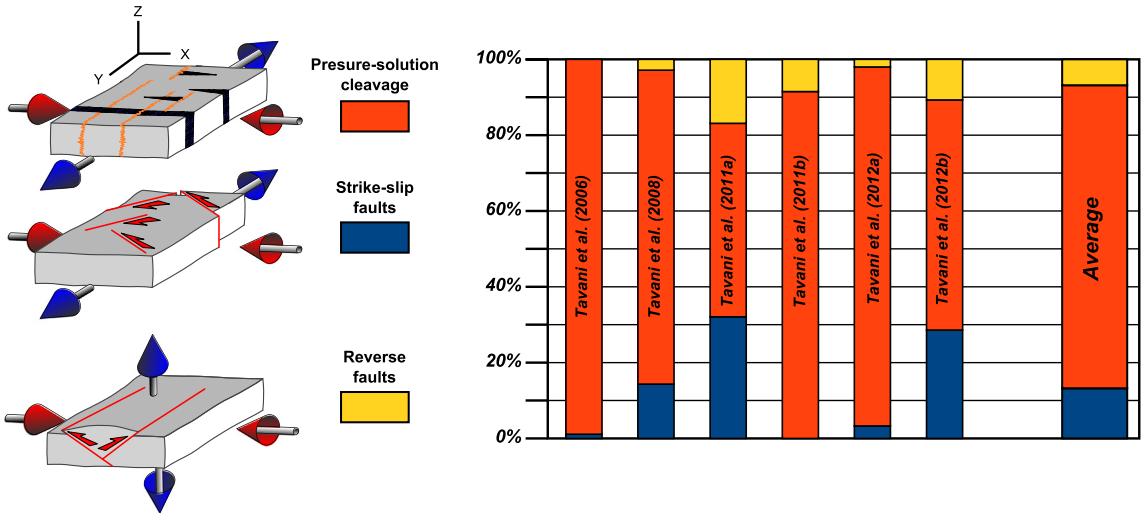

Fig. 8. Abundance, in carbonate strata of six reservoir-scale thrust-related anticlines, of structures developed during layer parallel shortening and associated with layer-parallel or layer perpendicular elongation. See text for details.

parallel outer-arc extension and inner-arc shortening along the direction perpendicular to the maximum curvature (Ramsay, 1967). The neutral surface commonly migrates during fold amplification (e.g. Ramsay, 1967; Frehner, 2011), causing the mutual overprinting of extensional and contractional domains through time. Within any mechanical layer, the local amount of strain scales with the distance from the neutral surface and is inversely proportional to the curvature's radius computed along the neutral surface itself (Fig. 9A). The total amount of tangential–longitudinal strain reduces when the bending material is modelled as a pile of mechanical layers separated by frictionless surfaces (Fig. 9B) (e.g. Fischer and Jackson, 1999; Hudleston and Treagus, 2010). This is because layers behave independently and the strain within each bed depends on the distance from its local neutral surface. Reducing the thickness of the layers implies a reduction of the maximum strain (Fig. 9). The graph in Fig. 9C also shows that in parallel folds involving well-layered strata with low-friction bedding surfaces, the maximum amounts of both extension and contraction occur in the inner sector of the fold, where the curvature radius is smaller. Of the two parameters that concur to determine the amount of tangential longitudinal strain, the curvature radius mainly relates with the large-scale thrust-fault architecture, whilst the thickness of the mechanical layer is essentially determined by the density of bedding-parallel slip surfaces and/or layers deformed by bedding-parallel simple shear (i.e. flexural slip and flexural flow, respectively; Donath and Parker, 1964; Ramsay, 1967; Chapple and Spang, 1974; Tanner, 1989). Thus, a well-layered sedimentary succession made of thin strata separated by low friction bedding surfaces will be weakly affected by tangential longitudinal strain. Conversely, in a massive carbonate unit made of poorly layered and thick strata, flexural-slip will be either inhibited or confined in some weaker layers. This causes the increase of the average thickness of the mechanical layers and, consequently, the amount of tangential-longitudinal strain. Indeed, in reservoir-scale thrust-related folds, several examples exist indicating fracturing and necking in tight and/or narrow fold hinge zones (e.g. Amrouch et al., 2010a; Bazalgette et al., 2010) where the layer thickness is only one or two orders of magnitude smaller than the curvature radius. Conversely, for more smoothed geometries where the curvature's radius exceeds hundreds or thousands of metres, the generally invoked fit between fracture density and

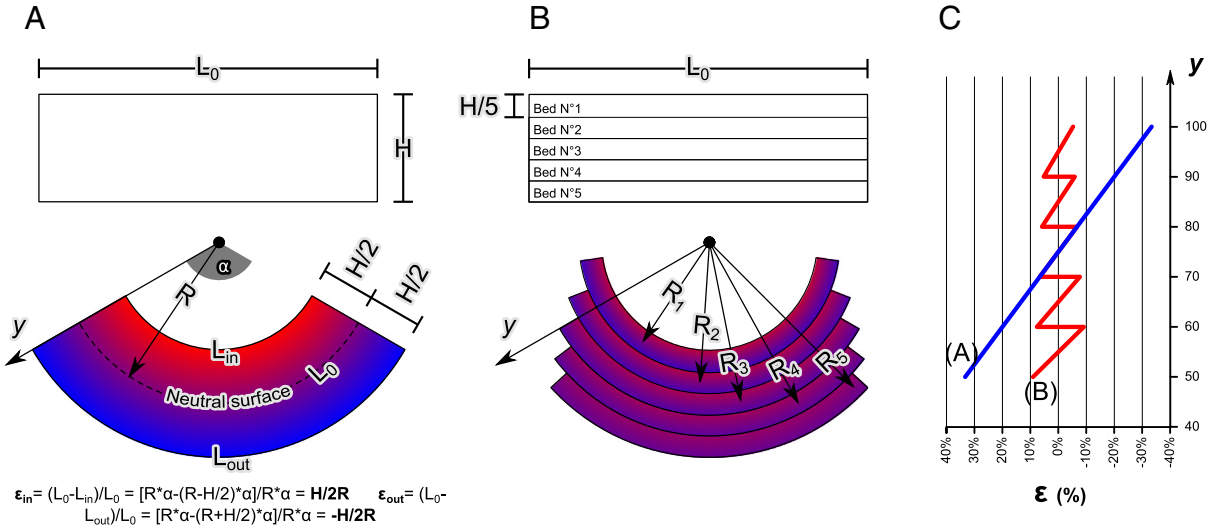

Fig. 9. Tangential–longitudinal strain associated with bending of a beam (A) and of a pile of beams having an equivalent thickness (B), with formulas relating maximum strain (in the inner and outer arcs), radius of curvature, and thickness of the beam. Red and blue indicate amount of shortening and elongation, respectively. (C) Amount of strain ad different distances from the centre of curvature for models A and B, showing how occurrence of layer-parallel discontinuities reduces the maximum amount of strain. (For interpretation of the references to colour in this figure legend, the reader is referred to the web version of this article.)

curvature is mostly an assumption rather than an observation. In fact, the existence of a relationship between curvature and strain is commonly documented in outcrop-scale folds (e.g. Maerten and Maerten, 2006) whilst it is documented for km-scale folds mostly in thick units (e.g. Evans and Elmore, 2006).

Curvature evolution and the associated deformation templates, are generally related to two main fold kinematics: fixed-hinge (e.g. De Sitter, 1956) and active hinge-folding (e.g. Suppe, 1983). In the first case (Fig. 10), folding is ensured by almost rigid limb rotation about fixed axial surfaces, across which negligible material migration occurs (e.g. De Sitter, 1956). Tangential–longitudinal strain and associated deformation occur in the hinge areas, with flexural slip being confined to the rotating limbs (Ramsay, 1974; Anastasio et al., 1997; Fischer and Jackson, 1999). The deformation pattern evolution during fixed-hinge folding is schematically illustrated in Fig. 10. During the early stages of folding, when the anticline has a gentle geometry and a large curvature radius, curvature-related deformation occurs in the thicker competent layers, whilst very small amount of flexural slip/flow occurs in weaker units. Increasing shortening implies limb rotation and progressive fold tightening. Bending-related strain continues to operate in the stiffer and thicker layers and progressively starts to affect also layers deforming by flexural slip. Contextually, the amount of bedding-parallel shear progressively increases.

Active or migrating hinge folding implies the migration of material through axial zones separating roughly homogeneously dipping rock panels (Fig. 11) (e.g. Suppe, 1983). Within the axial zone, bending of the migrating material causes deformation until it enters the adjacent constant dip domain, where the deformed material is passively carried out during further translation. Accordingly, the distribution of axial surfaces within folds growing by active-hinge folding is predicted to control the time-space evolution of deformation and, in particular, it would determine fold partitioning into different deformation domains (Sanderson, 1982; Evans and Dunne, 1991; Storti and Salvini, 1996; Salvini and Storti, 2001). The deformation pattern within active axial zones is similar to that expected within fixed axial surfaces, with the addition of flexural slip. Despite few field cases (Srivastava and Engelder, 1990; Maillot and Koyi, 2006), unequivocal evidence for the migration of material across active axial surfaces is rare because it is generally expected to produce only flexural slip-related deformation. This because, for km-scale thrust related anticlines, the radius of curvature in active axial surfaces is drastically higher that in fixed ones and, with few possible exceptions, the migration of material across active axial surfaces is expected to produce mostly bedding-parallel shear, whilst tangential longitudinal strain would be inhibited. This was, for example, documented in the hanging-wall ramp of the Pine Mountain Thrust by Wiltschko et al. (1985), who concluded that the acquisition of dip of the rocks on the ramp was primarily accomplished by bedding-plane

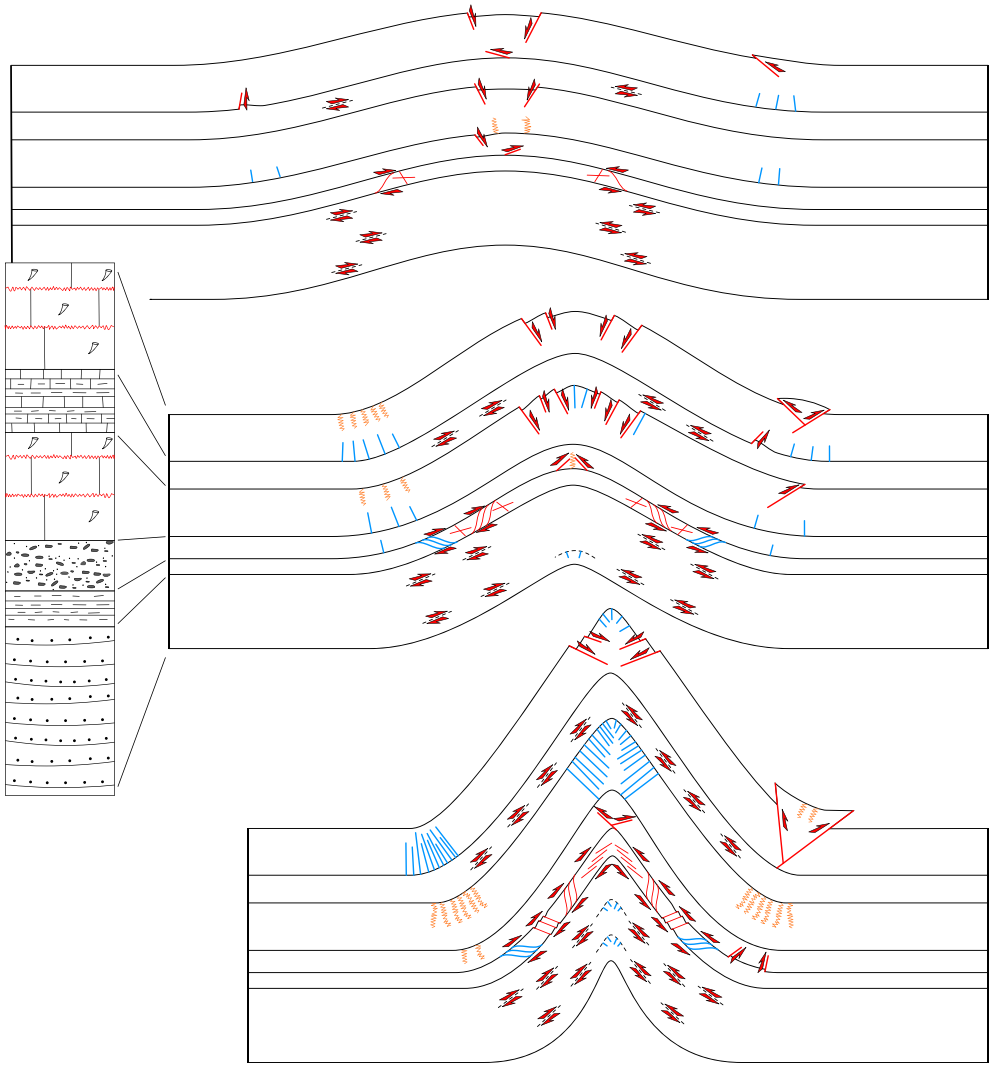

Fig. 10. Progressive evolution of the deformation pattern in a multilayer deformed by fixed-hinge folding, where tangential–longitudinal strain accumulates in the fixed hinge regions, whilst flexural-slip and flexural-flow related deformation occurs in the limbs of the fold.

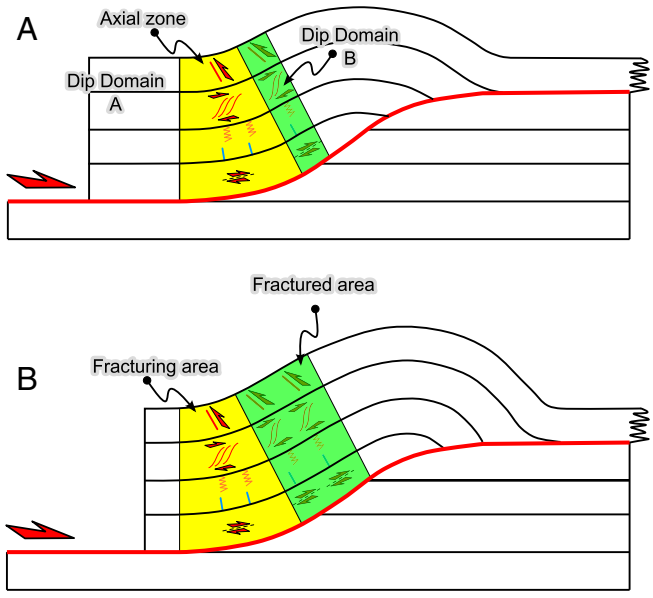

Fig. 11. Progressive evolution of the deformation pattern in a multilayer deformed by active-hinge folding, where tangential–longitudinal strain and flexural slip/flow occur when hanging-wall material migrates across a fixed (and active) axial surface.

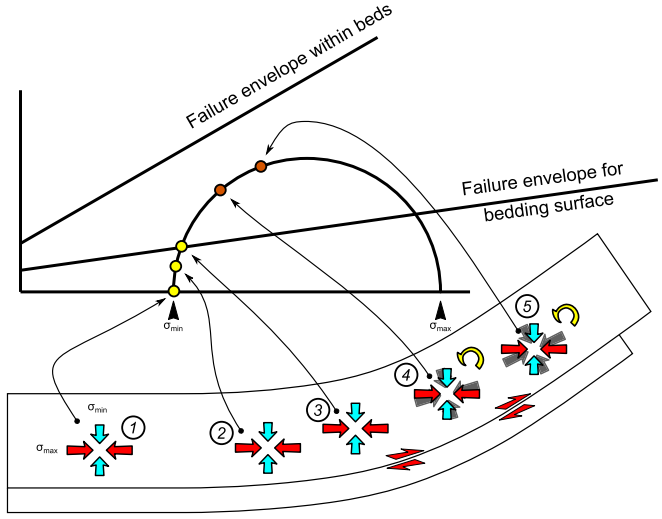

Fig. 12. Stress channelisation in well layered materials. Bedding surfaces is assumed to have both cohesion and friction significantly smaller than those of the beds. A stress component is assumed to be oriented parallel to the section, and the problem is addressed in 2D. Remote 2D maximum and minimum stress components are oriented horizontal and vertical, respectively, and their values are indicated in the Mohr–Coulomb diagram. Small circles indicate the state of stress of the bedding surfaces at different bedding dip values. Yellow circles indicates a sub-critical state of stress whilst after certain amount of dip, the bedding surfaces are in a supra-critical state, indicated by orange circles. To avoid continuous shearing and preserving at the same time the magnitude of the remote stress field components, the local stress has to reorient and, in particular, the maximum stress component must reduce its angle with respect to bedding. (For interpretation of the references to colour in this figure legend, the reader is referred to the web version of this article.)

slip on the slip surfaces which experienced a shear stress of < 100 bars [10Mpa]. Bending strains in units between slip surfaces were too small to alter the pattern of layer-parallel shortening preserved in the Newman Limestone. Accordingly, the occurrence of significant tangential–longitudinal strain supports fixed hinge folding.

2.4.2. Syn-folding layer parallel shortening

Wiltschko et al. (1985), still referring to the Pine Mountain Thrust area, also wrote that the calcite twinning results and observations on filled joints and slip surfaces in outcrop indicate that individual beds in the Newman Limestone acted more or less independently, with slip between layers allowing nearly layer-parallel shortening. The association between slip along bed surfaces and layer-parallel shortening in tilted strata during folding, relates with the fact that nearly frictionless, low cohesion interlayers support shear stresses that are much lower than those that are necessary to trigger intrabed shear. As a consequence, the stress tensor re-orients in the proximity of slipping surfaces (e.g. Ohlmacher and Aydin, 1997), in order to keep two of the principal axes parallel to bedding and the third one perpendicular to it (Fig. 12). Stress re-orientation during flexural slip folding has been invoked to explain the following field observations in the Northern Apennines (Tavani et al., 2012a): (1) pressure solution cleavage across the mountain front anticline reduces its frequency from the limbs towards the crest; (2) pressure solution cleavage surfaces are at high angles to bedding but not exactly bedding-perpendicular and, when bedding dip is restored to horizontal, the cleavage shows small deviations from the vertical that are opposite in the two limbs and are consistent with a top-to-the-hinge shear component (Fig. 13); and (3) the strike of pressure solution cleavage, both in its present orientation and after bedding dip removal, is slightly oblique to the trend of the anticline and is perpendicular to the tectonic transport direction provided by abundant S–C structures exposed along the underlying thrust. Observations 1 and 2 point to a syn-folding origin for the cleavage, whilst the third feature rules out any significant role of tangential longitudinal strain in cleavage development because the cleavage itself is not parallel to the strike of the fold axial surface. These observations indicate bedding-parallel stress channelling during folding, with the maximum stress orienting parallel to the regional shortening direction in map view and rotating in a vertical plane to maintain a low angle to bedding (Tavani et al., 2012a). Extensional deformation structures oriented perpendicular to both cleavage and bedding occur in many thrust-related anticlines developed in carbonate multilayers (Tavani et al., 2006a, 2008, 2011a, 2012a), indicating that σ_3 was oriented parallel to bedding and perpendicular to the tectonic transport direction. This stress configuration can be related with the occurrence of syn-folding along-strike stretching during fold lateral propagation and arching (e.g. Dietrich, 1989; Price and Cosgrove, 1990). When transport direction and fold axis are mutually perpendicular, it is not possible to discriminate the role of the along-fold stretching from that of the regional layer-parallel and shortening-perpendicular stress component. The few examples where field data show that the shortening direction is oblique to the strike of the anticlines indicate that the orientation of transverse syn-folding extensional deformation structures is mostly controlled by the regional stress field (Tavani et al., 2011a, 2012a). Accordingly, we can deduce that at least in the available case studies, the minimum principal axis of the stress ellipsoid σ_3 was, "regionally" sub-horizontal and oriented at low angle to the thrust during fold growth.

The mechanism of flexural slip can operate up to a certain value of bedding dip, typically less than about 60° (e.g. De Sitter, 1956; Ramsay, 1974; Gutiérrez-Alonso and Gross, 1999), and afterwards folds almost lock. This implies that the process of bedding-parallel stress channelling becomes progressively less efficient during limb rotation until it stops when slip along bedding surfaces terminates. At this stage, the cause of stress channelling is removed and the maximum principal axis of the stress field re-attains its regional, sub-horizontal, attitude also within the fold, as later discussed in the fold tightening section. The value of bedding dip at which stress channelling along bedding stops, largely depends on the frictional properties of the folded multilayer and can be derived from the angular relationships between syn-folding deformation structures and bedding dip. As an example, in the well-layered Umbria-Marche carbonate sedimentary pile of the Northern Apennines (Italy), we found that the angle between pressure solution cleavage and bedding remains constant after bedding dip values of about 30° that, accordingly, provides the upper limit for an effective stress channelisation (Tavani et al., 2012a).

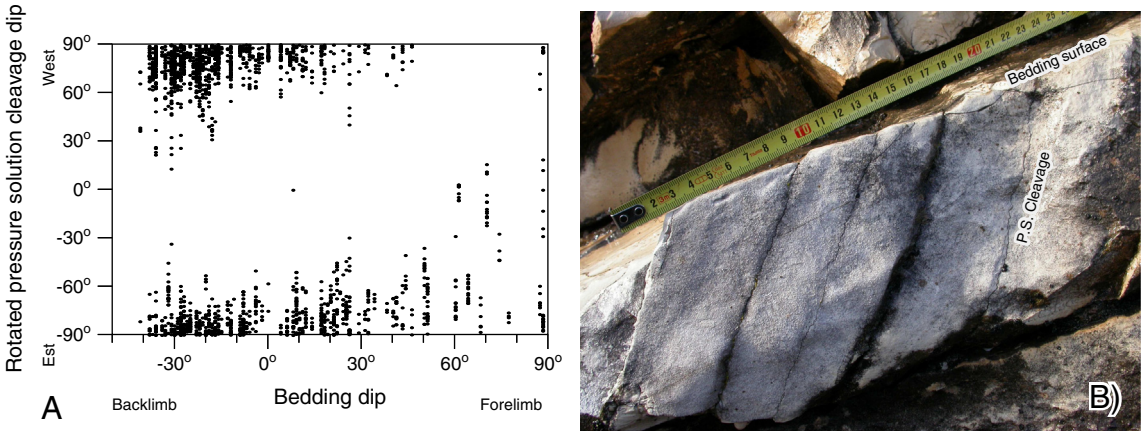

Fig. 13. (A) Variability of the angle between pressure solution cleavage and bedding surface at different bedding dip values across the mountain front anticline of the Northern Apennines (after Tavani et al., 2012a), with (B) photo showing an example of cleavages oriented obliquely to the bedding. The figure indicates how pressure solution cleavage tends to have opposite deviations from the bedding-perpendicular direction in the two limbs of the fold. This support a syn-folding origin and indicates stress channelisation, which stops at about 30°, as indicated by the rather constant angular relationships between cleavage and bedding after this bedding dip value.

2.4.3. Deformation ahead of the upward propagating fault tip and footwall syncline stretching

Folding ahead of propagating thrust ramps, i.e. fault-propagation folding, is probably the most common macro-scale mechanism to accommodate fault displacement in foreland fold-and-thrust belts (e.g. Dahlstrom, 1969; Faill, 1973; Elliott, 1976; Chapman and Williams, 1984; Suppe and Medwedeff, 1984). During fault-propagation folding, the multilayer is partitioned in faulted and unfaulted strata and, whilst in the former shortening can be entirely accommodated by slip along the thrust fault, unfaulted strata may require additional strain to accommodate shortening (Williams and Chapman, 1983). In the simplest model configuration, flexural slip and line-length preservation are imposed, with the above-mentioned additional deformation in the unfaulted layers being totally ensured by folding (Suppe and Medwedeff, 1990). This leads to user-friendly geometrical construction that, however, largely fails to reproduce well-constrained fault-propagation anticlines, as evidenced by the inconsistency between expected and observed inter-limb angles (e.g. Mitra, 1990) and by the occurrence of unnatural growth strata patterns consisting of several growth-triangles (e.g. Storti and Poblet, 1997). Several alternative solutions have been proposed to reproduce more natural fault-fold evolutions, all of them requiring internal strain of layers (Jamison, 1987; Chester and Chester, 1990; Mitra, 1990; Suppe and Medwedeff, 1990; Wickham, 1995; Tavani et al., 2006b). Among them, trishear fault propagation folding is increasingly applied. This mechanism, proposed by Erslev (1991) and later implemented by other authors (e.g. Hardy and Ford, 1997; Allmendinger, 1998; Mitra and Mount, 1998; Zehnder and Allmendinger, 2000; Cardozo et al., 2011), assumes that a triangular zone emanates from the upward propagating fault tip. Typically, layers within the triangular shear zone firstly undergo shortening and thickening, both progressively reducing with increasing fault throw and tilting of bedding, until the onset of layer-parallel stretching and thinning occurs. Although the trishear model is able to successfully reproduce the geometry and growth strata pattern of many natural folds, it basically neglects the role of layer-parallel anisotropies during folding. Such an extreme simplification may represent a valid assumption for many types of rock rheology, including those of poorly layered rocks and of both natural and numerical sandboxes, but it cannot be assumed as a general rule. In fact, the difficulty of applying trishear to the well-layered portions of folded packages has been pointed out, among others, by its inventor (Erslev and Mayborn, 1997). In contrast to trishear, double edge fault propagation folding (Tavani et al., 2006b) assumes a strong influence of layering during fold growth. In essence, this folding mechanism reproduces the triangular deformation zone of the trishear but it assumes that, within the deformation zone emanating from the fault tip, layer thickness is preserved and deformation entirely occurs by syn-folding layer-parallel shortening. This is itself an end-member behaviour, able to describe the deformation of well-layered materials, which can bear significant cross-sectional area loss during LPS. These two models, i.e. trishear and double-edge fault-propagation folding, apply to different mechanical stratigraphies, so that they are expected to operate together when alternating types of rheology exist. Importantly, both models predict that, in order to reproduce the natural shape of fault-propagation anticlines, additional strain is required ahead of the propagating fault tip. In agreement with this, perturbation of the stress and strain patterns ahead of the upward propagating fault tip is expected. Indeed, this kind of stress and strain perturbation has been documented in many km-scale fault propagation anticlines (e.g. Bellahsen et al., 2006b; Tavani et al., 2006a; Amrouch et al., 2010a; Beaudoin et al., 2012), essentially in agreement with the fact that almost layer-parallel shortening is imposed during the early stages of fault propagation, accompanied by either along-strike or vertical elongation.

Although in different ways, both in trishear and double-edge fault propagation folding the development of a footwall syncline may occur. A given layer, which has firstly experienced shortening, with approaching the fault tip becomes part of the footwall syncline and experiences layer-parallel stretching and thinning. This can be particularly intense in the footwall syncline of trishear fault propagation anticlines (e.g. Mitra and Miller, 2013), as documented by extensional structures accommodating layer-parallel stretching in the synclinal areas underlying the main thrust ramp (e.g. Gutiérrez-Alonso and Gross, 1999; McQuarrie and Davis, 2002).

2.5. Fold tightening

A fold grows until limb rotation and strata curvature cannot accommodate shortening anymore. At that stage, which reflects a kind of "locking" of the fold, the rock mass still undergoes shortening, but the contraction that initiated the fold is now oriented at a high angle to bedding. This leads to a late stage of fold tightening during which strata are not tilted anymore and shortening is accommodated by deformation structures that cut across the strata irrespective of bedding dip. They are typically fore-thrusts and back-thrusts occurring respectively in the forelimbs and backlimbs of folds (e.g. Gutiérrez-Alonso and Gross, 1999; Tavani et al., 2008), bedding-parallel pressure solution cleavages offsetting pre- to syn-folding deformation structures (e.g. Tavarnelli, 1997), or conjugate strike-slip faults recording a sub-horizontal

maximum principal axis of the stress ellipsoid (e.g. Allmendinger, 1982; Tavani et al., 2008; Amrouch et al., 2010a, 2011; Casini et al., 2011; Lacombe et al., 2011; Beaudoin et al., 2012). It is worth noting that, in many cases, thrusts occurring during fold tightening are formed by strands of reactivated inherited syn-orogenic deformation structures (e.g. Tavani et al., 2008; Petracchini et al., 2012), which link to form a larger fault.

2.6. Gravity driven extensional deformation

During thrusting and folding in the foredeep and foreland basin of thrust-fold belts, the dip of the regional monocline and the associated subsidence rate determine either a positive or a negative fold total uplift (Doglioni and Prosser, 1997; Doglioni et al., 1999). Positive uplift can trigger gravity-driven deformation that mostly affects the shallower portions of fold limbs (e.g. Morley, 2007; Laird and Morley, 2011) or strongly plunging periclinal areas (Guillaume et al., 2008), where longitudinal and transverse extensional faults develop, respectively. Whilst such well-developed extensional faults are predominantly a deepwater fold feature, there are also few examples of extensional faults affecting anticlines in continental settings, triggered by gravity (e.g. Tavani et al., 2014).

2.7. Role of structural inheritance

Structural inheritance can make difficult the unequivocal identification of the relative chronology among deformation structures because crosscutting and abutting relationships can be significantly altered during multiple reactivations. Moreover, both field investigations (Bergbauer and Pollard, 2004) and geomechanical models (Guiton et al., 2003a,b; Sassi et al., 2012) suggest that re-activation of pre-folding deformation structures, whatever their origin, may inhibit the development of classical folding-related deformation patterns.

In the frontal region of orogenic systems, underthrusting of the lower plate causes translation of rock containing transverse joints, formed during along-strike stretching, into the LPS domain. There, they can provide properly oriented mechanical discontinuities able to favour precipitation of calcite removed by pressure solution. Accordingly, it may be argued that veins nearly perpendicular to both bedding and pressure solution cleavages, could actually result from inherited joint re-opening perpendicularly to σ_2 rather than new tensile extensional fracturing. This inference, however, is partly confuted by the observation that pressure solution cleavages and transverse veins frequently display mutual cross-cutting relationships, indicating their synchronous development. This evidence indicates that, although many transverse veins associated with pressure solution cleavages could have been inherited from the previous along-foredeep stretching or foreland-flexuring stages, their re-opening occurs in a stress field where σ_3 remains sub-horizontal.

When the shortening direction is roughly perpendicular to the trend of the foredeep/peripheral bulge system, σ_1 strikes perpendicular to foreland-flexure-related longitudinal extensional deformation structures when they enter the LPS domain, thus ruling out any possible strike-slip reactivation. Inherited longitudinal joints can be reactivated as pressure solution surfaces (Railsback and Andrews, 1995). Depending on their strength (Sibson, 1985, 1995), longitudinal faults can: (i) be not reactivated, (ii) induce buttressing, (iii) be positively inverted, or (iv) exhibit mixed behaviours (e.g. Coward et al., 1989; Glen et al., 2005) (Fig. 14). Poor LPS-related deformation occurring in a strike-slip stress field configuration, with no positive inversion of foreland-flexure extensional faults, is described in the Khaviz anticline of the Zagros (e.g. Wennberg et al., 2006). Buttressing against foreland-flexure-related extensional faults is documented when they cut across several layers or approach a basin scale size (e.g. Scisciani et al., 2002). Buttressing can also produce overprinting of fault surfaces by pressure solution, and creation of slickolites (Tavani et al., 2012a). Three scenarios may be envisaged for positive fault inversion (Fig. 14): (1) it occurs whilst LPS produces little or no deformation structures; it occurs whilst LPS produces significant deformation structures associated with either sub-vertical σ_2 (2) or σ_3 (3). The first case has been described in the Boltaña anticline of the Spanish Pyrenees (Tavani et al., 2012b), where only few of the abundant foreland-flexure extensional longitudinal faults have been positively inverted and compressional deformation structures rarely occur. Case 2 is that of the Northern Apennines where, with few local exceptions, layer parallel shortening has occurred in a strike-slip stress field configuration (Tavani et al., 2008, 2012a). In that area, foreland-flexure extensional faults are described (Tavarnelli and Peacock, 1999) and few of them have been inverted (Tavani et al., 2012a). The same has been documented in the foreland area ahead of the Cantabrian domain of the Pyrenean Orogen (Quintà and Tavani, 2012), where positive inversion of foreland flexure extensional faults occurred both in the presence of pressure solution cleavages/strike-slip faults (i.e. case 2) and in the absence of any compressive/strike-slip structure (case 1).

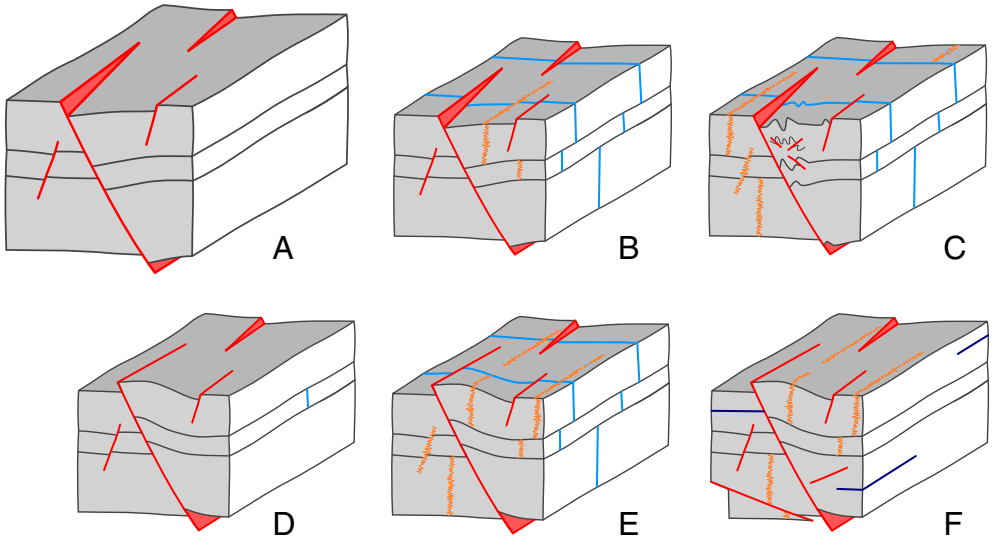

Fig. 14. Examples of possible relationships between LPS pattern and behaviours of inherited longitudinal extensional faults. A) Pre-LPS extensional fault pattern. B) Faults are not reactivated and LPS occurs with a near vertical σ_2. C) Few faults induce buttressing and LPS occurs with a near vertical σ_2. D) Few faults are positively inverted, whilst no fracturing occurs in the surrounding material. Few faults are positively inverted or reactivated as pressure solution cleavage, and LPS occurs with a near vertical σ_2 (E) or near vertical σ_3 (F).

Thrusting and onset of previously described syn-folding deformation implies that early-orogenic structures, including those developed during pre- to early-folding LPS, are tilted together with layers and can undergo reactivation, typically by positive inversion of inherited longitudinal extensional deformation structures and by further compression or shearing of deformation structures developed during the LPS stage. Syn-folding tangential longitudinal strain induces outer-arc extension and inner arc compression, and this can imply: (1) extensional reactivation of inherited longitudinal extensional structures; (2) extensional reactivation of inherited compressional structures developed during LPS (i.e. longitudinal reverse faults and longitudinal pressure solution cleavages); (3) contractional/strike-slip reactivation of inherited contractional/strike-slip structures developed during LPS; and (4) positive inversion of inherited longitudinal extensional structures. Similarly, during fold tightening and footwall syncline stretching, inherited longitudinal structures become favourably oriented with respect to the active stress field, allowing for their reactivation. In essence, field evidence indicates that during folding the inherited longitudinal compressional and extensional structures may undergo both extensional and compressional reactivation (e.g. Graham et al., 2003; Bellahsen et al., 2006a; Amrouch et al., 2010a; Beaudoin et al., 2012; Tavani et al., 2012b), whilst conjugate strike-slip faults can undergo only strike-slip reactivation, with the syn-folding reactivation of pre-folding structures inhibiting the development of syn-folding sensu strictu deformation structures.

Occurrence of pre-orogenic deformation structures can further modify, and make more complex, the deformation patterns illustrated above. The simplest case is one in which inheritance includes deformation structures oriented approximately parallel and/or perpendicular to the trend of the foredeep-belt system. In this case, inherited structures can be reactivated with an extensional kinematics during foreland flexuring and/or along foredeep stretching. During the pre-folding and the syn-folding LPS stages, the reactivation scenarios illustrated for the early orogenic extensional deformation structures also apply to these pre-orogenic inherited ones. An example is provided by the Bristol Channel (e.g. Dart et al., 1995; Nemčok et al., 1995; Kelly et al., 1999), where pre-orogenic inherited faults are almost perpendicular to the shortening direction and buttressing and positive inversion is accompanied by the development of reverse and, mostly, strike-slip faults. Another example involving pre-orogenic extensional structures oriented almost perpendicular to the shortening direction is the Cotiella extensional rollover in the Pyrenees (Tavani et al., in press). There, the dense network of inherited extensional faults and joints has been tilted during basin inversion and only very few faults show evidence of positive inversion. More complex are all those frameworks in which structural inheritance is oblique to the convergence direction, as a wide range of scenarios spanning from oblique inversion to fully strike-slip reactivation can occur. As an example, in the Sant Corneli-Boixòls oblique inversion anticline of the Spanish Pyrenees, pre-orogenic extensional faults are widespread and strike at about 45° to the shortening direction. Positive inversion of the basin-boundary buried fault zone caused strike-slip reactivation of inherited deformation structures, synchronously with the development of transverse veins and joints, and rare pressure solution cleavages. This pattern indicates that fault inversion was accompanied by a "weak" LPS, occurring in a strike-slip stress field configuration (Tavani et al., 2011a). A similar oblique framework is observed in the outer portion of the western Pyrenean Orogen, in the Cantabrian Mountains (Quintà and Tavani, 2012). Widespread extensional features developed during foreland flexuring and along-foredeep stretching are preserved in this area and strike perpendicular and parallel to the shortening direction, respectively. These early-orogenic deformation structures tend to rotate when approaching pre-existing fractures and their angle to the shortening direction becomes about 20–30°, instead of 45°. This behaviour indicates that structural inheritance can locally influence the orientation of a newly developed stress field (Bergbauer and Pollard, 2004). On the other hand, the inherited deformation pattern appears to have no effect on the stress field orientation during the subsequent LPS stage, when it underwent strike-slip reactivation (Quintà and Tavani, 2012). In the same region, but in an innermost position within the belt, two mutually orthogonal sets of pre-orogenic extensional faults and joints form an angle of about 20–30° and 60–70° with the shortening direction, respectively. They were re-activated as extensional features during foreland flexuring and along-foredeep stretching, and as strike-slip faults during shortening, and prevented development of newly formed deformation structures (Tavani and Muñoz, 2012).

Structural inheritance can occur only at specific levels of sequences undergoing contraction (typically the lower part and/or the basement), favouring vertical decoupling of stress and strain patterns (e.g. Keating et al., 2012). Furthermore, thrust development by re-activation and linkage of obliquely striking pre-orogenic deformation structures can induce local stress and strain patterns only in the folded areas surrounding the reactivated structures (e.g. Ahmadhadi et al., 2008; Carminati et al., 2013). Analogously, whatever their origin, salients, recesses, and oblique-lateral ramps, can induce local progressive rotations of both stress field and inherited early-orogenic to early folding deformation structures, so that complex but local reactivation patterns are expected in these areas.

2.8. Paleostress regimes from striated faults in fold-thrust belts

Whatever technique is used (e.g. Célérier et al., 2012) to invert fault slip data, and despite the still ongoing debate on whether these methods actually provides information on either stress or strain, or even strain rates (e.g., Twiss and Unruh, 1998; Lacombe, 2012), a wealth of paleostress reconstructions have been carried out worldwide in various tectonic settings over the last decades, providing results that are consistent with the orientations of related stylolites and joints (e.g. Sperner and Zweigel, 2010; Lacombe, 2012).

The compilation of Lisle et al. (2006) shows a steeply plunging principal axis of the paleostress fields obtained in most reconstructions, thus validating the classical hypothesis of Andersonian stress regimes. As stated before, in weakly deformed forelands Andersonian faulting is supported by widespread near vertical jointing, a condition that is most likely if one of the principal axes of the stress ellipsoid is vertical. On the other hand, in fold-thrust belts, where deformation intensity is much higher, even though the far-field stress is of Andersonian type, numerical models show an increased complexity caused by the evolution of flexural-slip folding of multilayers with variable mechanical stratigraphy (e.g. Sanz et al., 2008). In particular, stress field inversion supporting the inference of a principal axis of the stress ellipsoid perpendicular to bedding and the other two lying on the bedding surfaces, yield Andersonian environmental conditions only after unfolding, which in turn implicitly leads to consider them as pre- or early-folding.

Although this view has provided in most cases reliable first-order geodynamic interpretations, the well-known occurrence of bedding-parallel stress channelling (e.g. Mandl, 2000) implies possible deviations from Andersonian conditions, at least at the scale of thrust-related folds. Such an ambiguity is not easy to resolve, as indicated by the case of NW Taiwan, where analysis of striated small-scale thrust faults and bedding parallel slip surfaces, both in their current orientations as well as after bedding restoration to the horizontal (unfolding), always provided a sub-horizontal σ_1 (Lacombe et al., 2003).

Regardless of the relative timing of faulting and folding, it is interesting to note that paleostress inversion techniques commonly provide a near bedding-parallel σ_1 paired with a variability of the orientation of σ_2 and σ_3. In the Taiwan case, σ_2 is commonly vertical, therefore indicating a strike-slip stress field configuration during thrust emplacement in regions where the trend of the mountain front relative to the regional compression is oblique and/ or in regions undergoing incipient lateral extrusion like SW Taiwan. In contrast, near vertical σ_3 is obtained in regions where pre-orogenic extensional basins are inverted (Mouthereau et al., 2002).

Another evidence for switching between the minor and intermediate axes of the stress ellipsoid within orogenic systems is provided by the Bighorn basin within the Laramide belt in western USA, as documented in multiple works (e.g., Varga, 1993; Erslev and Koenig, 2009; Neely and Erslev, 2009; Amrouch et al., 2010a; Beaudoin et al., 2012; Weil et al., 2014). At the regional scale, the fault pattern includes conjugate dip-slip reverse faults at acute angles to bedding, which accommodated minor LPS and vertical thickening, and conjugate strike-slip faults at high angles to bedding that accommodated minor LPS and belt-parallel extension, both systems indicating an early LPS, prior to and synchronous with initial arch development. Estimated stress ratios are generally low, indicating similar magnitudes of σ_2 and σ_3. At the scale of individual structures, more detailed analyses document also late- to post-folding fault arrays that still support the occurrence of both compressional and strike-slip stress field configurations (Amrouch et al., 2010a; Beaudoin et al., 2012). In the Fars province of the Zagros belt (Iran), paleostress reconstructions using striated faults reveal the presence of both compressional and strike-slip stress field configurations in response to the Neogene and still ongoing collision of the Arabian and Eurasian plates. This coexistence accounts for the kinematics of the major faults and for the combination of strike-slip and thrust-type focal mechanisms of earthquakes whatever their magnitudes and focal depths, and whether they occur in the sedimentary cover or in the basement (Lacombe et al., 2006). The inversion of fault-slip data also reveals low stress ellipsoid shape ratios (being defined as $[\sigma_2 - \sigma3]/[\sigma_1 - \sigma3]$), which suggests that σ_2/σ_3 permutations allow for the coexistence of compressional and strike-slip regime with a nearly constant sub-horizontal $\sigma1$. Very similar results were obtained by using microstructures such as calcite twins (Lacombe et al., 2007).

In the Jura region of the Alps (eastern France–Switzerland), the stress field evolution induced by the Miocene compression was studied in detail by Homberg et al. (1999, 2002). The authors show that, before folding, there was a strike-slip stress field configuration with a fan-shaped distribution of σ_1 trajectories related to the indentation of the future Jura domain by its hinterland. In contrast, during and after the main folding phase, the stress configuration remained of strike-slip type in the flat-lying and weakly deformed parts of the external Jura ("Jura des Plateaux"), whilst in the internal part of the belt ("Folded Jura") and near to major thrusts of the external Jura, a replacement by a compressional or transpressional stress configuration occurred.

From this brief description above we note the widespread occurrence, and even prevalence, of strike-slip stress configurations within thrust-fold belts and their forelands, away from major thrust systems.

3. Discussion

Following from field evidence presented in the previous sections, we now attempt to reconstruct the stress field evolution for a given volume of a fully lithified carbonate-dominated sedimentary succession, from the foreland flexuring stage to thrust fault nucleation and fold amplification (Fig. 15). For this purpose, we use the equations of linear elasticity linking stress and strain in isotropic and homogeneous materials (e.g. Turcotte and Schubert, 1982; Price and Cosgrove, 1990), which are illustrated in Fig. 16A. In the pre-orogenic stress field configuration, the overburden load is the only significant acting force and, accordingly, σ_1 is vertical, i.e. parallel to the Z axis of our coordinate frame (i.e. Fig. 15A, time T0). No significant lateral rock expansion is allowed along X and Y directions and, assuming that inelastic deformation is negligible at this stage, it follows from equations 1 to 4 in Fig. 16A that sub-horizontal σ_2 and σ_3 have the same magnitude. The onset of tangential–longitudinal strain due to foreland flexuring (Fig. 15A, time T1) and, possibly, slab pull (e.g. Conrad and Lithgow-Bertelloni, 2002), causes the reduction of σ_x (equation 3 in Fig. 16A), which becomes the minimum stress and may attain negative values. During this stage the magnitude of σ_z remains approximately unaltered, whilst that of σ_y slightly reduces (less than that of σ_x) due to the influence of the negative σ_x (equation 4 Fig. 16A). Accordingly, during this stage σ_z and σ_y are the principal axes σ_1 and σ_2 of the stress ellipsoid, respectively. The onset of inelastic deformation, mostly consisting of longitudinal jointing, veining and faulting, can alter the relationships between the increment of ε_x and the variation of σ_x and σ_y, possibly inhibiting the decrease of the latter. At this stage, permutations between σ_y (σ_2) and σ_x (σ_3) are allowed only at the local scale because of joint-associated stress release (Hancock, 1985; Bai et al., 2002) and/or release faulting (Destro, 1995). Approaching the compressive deformation front (time T2 in Fig. 15A) the elastic portion of the previously acquired negative ε_x is progressively removed and σ_x tends to increase, possibly recovering its pre-orogenic value when the contribution of slab pull was negligible. Contextually, the vertical load (σ_z) increases because of sedimentation and infill of the foreland basin. The considered rock volume then enters into the layer-parallel shortening domain, where X-directed shortening (i.e. positive ε_x) causes an increase of σ_x, which firstly becomes the principal axis σ_2 at stage T3, and then σ_1 at stage T4. If along-strike stretching occurs between the foreland flexuring stage and the LPS stage, a negative stress component is added along the Y-axis, and the switching between σ_2 and σ_3, with the latter possibly becoming negative, occurs before the material starts to undergo LPS. Accordingly, at time T4 (Fig. 15A) the stress field configuration is strike-slip as σ_z is greater than σ_y. The site (i.e., X-position) where this permutation occurs depends on the vertical load, and on the depth.

Now let us consider what happens after T4 by using two end-member behaviours, involving elastic and inelastic deformation pathways (e.g. Guiton et al., 2003a). In the first case, shortening and stress building up along the X-direction imply expansion along the Y-direction that, as the material is laterally confined (or as soon as lateral expansion exceeds along-foredeep stretching), causes the increase of σ_y (equation 4 of Fig. 16A) until interchange between σ_y and σ_z occurs, and σ_y becomes the intermediate principal axis of the stress ellipsoid σ_2, whilst σ_z becomes σ_3 (T5 in Fig. 15A). The position within the orogenic system where this permutation occurs depends on ε_x, the vertical load, and the elastic properties of the rocks (i.e. Young's modulus and Poisson ratio) (equation 4 of Fig. 16A). Quite similar is the path followed in the second case, where permanent deformation occurs. In fact, after time T4 (Fig. 15A) the increase of ε_x leads to strike-slip faulting and, particularly in carbonate layers, development of pressure solution cleavage and related veins. Both types of inelastic deformation cause: (1) energy dissipation, which has the effect of reducing the ratio between stress and strain increment along the X-direction; (2) expansion of material along the Y direction (Fig. 16B), which produces an increase of σ_y until it equals σ_z at time T5. Further increase of σ_y during inelastic deformation is ensured by the occurrence of previously developed strike-slip faults and transverse joints. In fact, there is a transitional area where, although the stress configuration is compressive, reactivation of strike-slip faults containing σ_z (i.e. σ_3) is more favourable with respect to the development of new reverse faults containing σ_y (i.e. σ_2) (Fig. 16B). Similarly, the occurrence of bedding-perpendicular, low cohesion joints can favour the re-opening of the transverse set, oriented perpendicular to σ_y (i.e. σ_2) instead of the formation and subsequent mineral infilling of bedding-parallel joints. According to the field evidence from several thrust-related anticlines that the compressive stress configuration has never been reached, we suggest that major thrusting can occur either somewhere in between T4 and T5 or slightly after T5, i.e. both in strike-slip and compressive stress configurations. This is, for example, consistent with earthquake data from the Zagros, where coeval reverse and strike-slip faulting is documented at depth (e.g. Hessami et al., 2001).

Let us now consider the effect of folding-related deformation mechanisms on the two possible states of stress, i.e. compressive and strike-slip (Fig. 15B). In thrust-related anticlines oriented approximately perpendicular to the regional transport direction, inner-arc compression, fold tightening and compression ahead of the propagating fault tip, imply the local increase of σ_x and σ_y both during elastic and inelastic deformation. If the

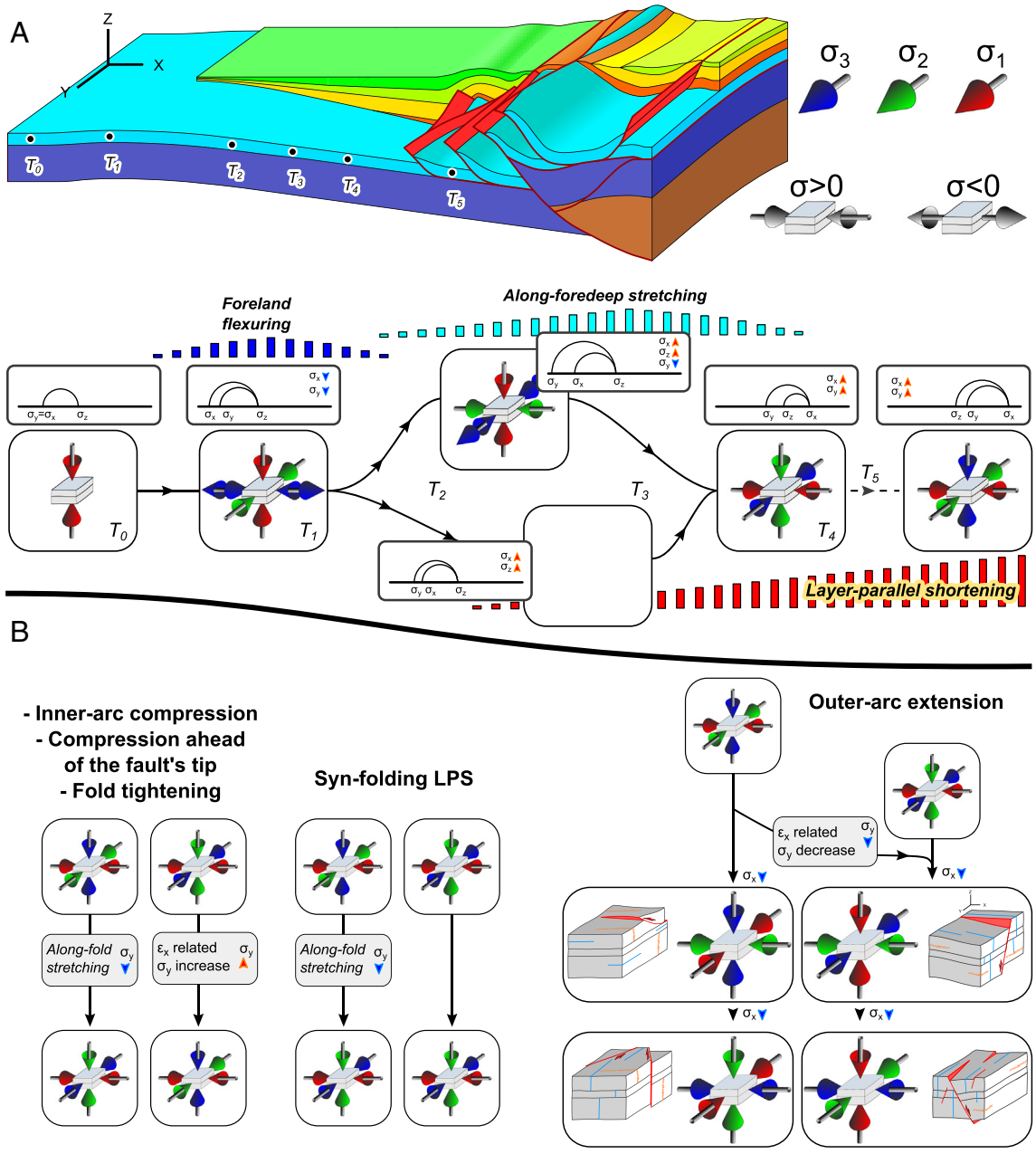

Fig. 15. Summary of the typical stress evolution during foreland fold and thrust belt development, before (A) and during (B) thrusting.

state of stress is of strike-slip type, the mechanisms discussed above can locally turn it into a compressive state, due to the effect that an increase of ε_x exerts on σ_y. Possibly, axis-parallel stretching generated by development of folds with curved hinge lines, can operate against the permutation between σ_2 and σ_3. If the state of stress is of compressive type, inner-arc compression, fold tightening and compression ahead of the propagating fault tip simply imply an increase of the maximum acting stress. If along-fold stretching occurs, the state of stress can become strike-slip. In the case of syn-folding LPS (Fig. 15B), minor modifications can occur, as the overall magnitude of σ_x changes slightly during folding. In the case of hinge-perpendicular stretching associated with outer-arc extension in a strike-slip regional stress field configuration, reduction of ε_x causes the reduction of σ_x until this stress component switches to σ_2 and σ_z becomes σ_1 (Fig. 15B). Transversal extensional faults, joints, and veins, oriented perpendicular to the fold strike, may develop at this stage. A further decrease of ε_x leads σ_x to eventually become smaller than σ_y, which becomes the intermediate principal axis of the stress ellipsoid σ_2, whilst σ_x becomes σ_3. Longitudinal extensional deformation structures can form at this stage. When the starting stress configuration is compressive, according to equations 3 and 4 (Fig. 15A) the reduction of ε_x causes a decrease of both σ_x and σ_y, with the latter becoming smaller than the vertical load sooner than the former. As a consequence, the reduction of ε_x turns the stress state into a strike-slip configuration and for further decreases of ε_x the stress field evolution follows that described above. However, this is valid only if no permanent deformation has occurred before hinge-perpendicular extension and the stress–strain relationships are entirely determined by elastic laws, which is a very crude oversimplification. The opposite end-member framework is one in which X-directed shortening has been mostly accommodated by inelastic deformation and the increase of σ_y has been mostly achieved by the inhibition of Y-directed expansion produced by strike-slip faulting and pressure solution cleavage-vein development (Fig. 16B). In this case, the reduction of σ_y requires the reactivation, with opposite senses of motion, of strike-slip faults, a field case that has not yet been reported, indicating that the reduction in the magnitude of σ_y during hinge-perpendicular extension almost entirely relies on the elastic part of the system, which is

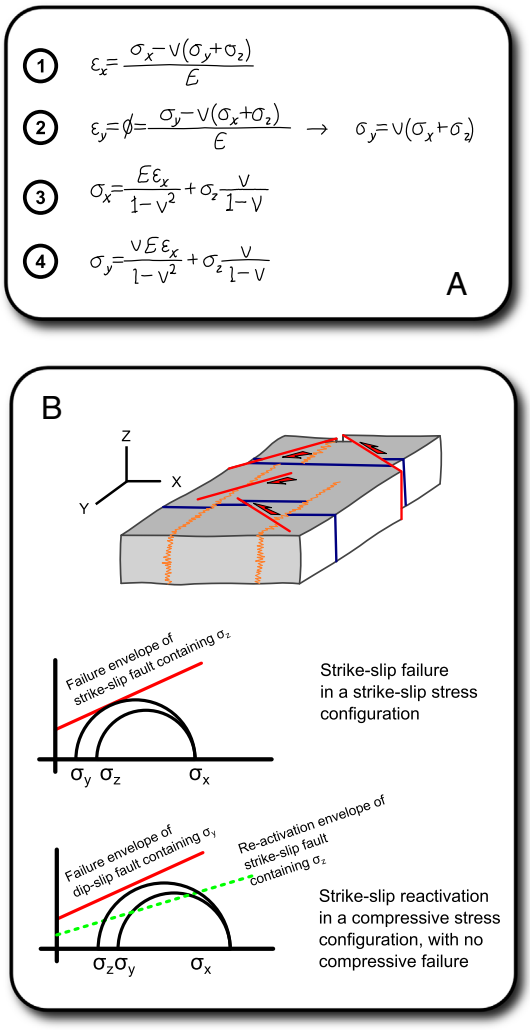

Fig. 16. Mechanisms of stress build-up. A) Equations 1 and 2 provide the elastic stress–strain relationships for a material confined along the Y-direction (i.e. $\varepsilon_y = 0$), where increment of ε_x causes the increment of both σ_x and σ_y. Combining equations 1 and 2 provides equations 3 and 4, where stress components are the explicit parameters. B) Inelastic stress build-up. In a strike-slip stress configuration, X-directed shortening achieved by strike-slip faults in a laterally confined material implies increase of σ_y. This mechanism continues to operate also when the stress configuration becomes compressive, as when minimum and intermediate stress components have close values the re-activation of strike-slip faults can be more favourable than development of new reverse faults.

not the dominant one. Accordingly, when σ_y greatly exceeds σ_z hinge perpendicular stretching can cause the interchange between σ_1 and σ_2, with σ_x becoming σ_2 and σ_y becoming σ_1, without being preceded by an early permutation between σ_y and σ_z. Reverse faults and pressure solution cleavages accommodating along-strike compression, possibly accompanied by the development of sub-horizontal veins, could form at this stage, particularly in the case of fluid-assisted deformation. A further decrease of σ_x would lead it to become the minimum principal axis of the stress ellipsoid σ_3, whilst σ_z becomes σ_2. Accordingly, strike-slip faults accommodating along-strike shortening would form. It is worth mentioning that, despite their mechanical feasibility, the along-strike compressional deformation structures predicted above are not common in thrust-related folds (e.g. Price and Cosgrove, 1990). This may relate to: (1) the axial parallel principal axis of the stress ellipsoid has always magnitudes that do not allow extensional and shear failure; however pressure solution cleavage development should develop in carbonate rocks and this makes option 1 quite unlikely; (2) fold axial stretching always ensures an early switching between the minimum and the intermediate stress axes, a possibility that is not favoured in the cylindrical or sub-cylindrical portions of folds, where axial stretching is expected to be negligible; (3) the stress field configuration is never of compressive type, or (4) it is of compressive type but inelastic deformation during stress build up is negligible and the decrease of ε_x during hinge-perpendicular stretching rapidly drives the stress configuration to a strike-slip type. Options 2, 3 and 4 appear to be more reasonable. This means that the onset of thrusting can occur in a compressional stress field configuration where, at the scale of the fold, the difference between the minimum and intermediate principal axes of the stress ellipsoid should be sufficiently small to allow either the "elastic" discharge of ε_x or the along-fold stretching to cause a decrease of σ_y down to its rapid permutation with σ_z.

Following the discussion above, it may be suggested that, during thrusting, the hanging wall material experiences a near subcritical state of stress that can have either a strike-slip or compressional configuration but, in the latter case, the difference between the magnitude of the minimum and intermediate principal axes of the stress ellipsoid is likely to be small. The key to understand how a thrust fault can nucleate in a strike-slip stress configuration is the state of stress during the LPS stage. Consider a layered material undergoing X-directed layer-parallel shortening above a sub-horizontal layer parallel décollement (Fig. 17A). The amount of X-directed shortening at the right edge of the model ($x = 0$) is D and remains constant along the vertical direction. At a certain position ($x = L$), the displacement along the décollement has been entirely accommodated by both reversible and irreversible deformation. Accordingly, the integral of the strain along the X direction, computed between 0 and L, must be equal to D in all the layers (equation 5 of Fig. 17B). It is intuitive that for the same stratigraphic level (i.e. at a constant depth) the amount of X-directed strain must reduce forelandward (equation 6 of Fig. 17B), as supported by field observations (e.g. Holl and Anastasio, 1995; Sans et al., 2003). Moreover, to avoid hinterland-ward layer-parallel shear, which is infrequently reported in foreland areas, the sum of strain accumulated at a given x coordinate (x1) must increase or remain constant as depth increases (equation 7 of Fig. 17B). In agreement with equations 5 to 7, the vertical profile of $\varepsilon_x = 0$ can have and hinterland-ward concave shape, imposing that the maximum ε_x in the inner side of the multilayer can increase downward (Fig. 17C). If we assume that in the outer sector of the model and with the exception of the uppermost unlithified stratigraphic layers, inelastic deformation does not take place, imposing $\sigma_x = \sigma_z$ in equation 3 allows one to derive ε_{xs} (equation 8 in Fig. 17B), i.e. the strain value at which a strike-slip stress configuration starts to be active. The hinterlandward increasing value of ε_x (Fig. 17C) and the dependence of ε_{xs} on the elastic parameters of the rocks, impose that the transition from extensional to strike-slip stress configurations can have a saw-tooth shape and hinterland-ward dipping cross-sectional profile (Fig. 17D). A similar behaviour cannot be inferred for the transition between strike-slip and compressional stress field configurations. In this case, in fact, it must be remarked that: (1) in the inner sector of the model, strain can increase downward (Fig. 17C); (2) in the strike-slip sector, irreversible deformation occurs, thus preventing the possibility to apply linear elasticity. The combined effect of these processes can lead to a foreland-dipping boundary between strike-slip and dip-slip stress configuration domains (Fig. 17D). Also in this case a saw-tooth shape is expected, being produced by the alternance of different mechanical units. In essence, and depending on the mechanical properties of the layers, it is possible to predict the presence of a compressional stress field configuration for some layers at depth, overlain by a wide volume dominated by a mostly strike-slip stress configuration. In addition, layer-parallel decollements may have a variable dip controlled by the foreland regional monocline (e.g. Mariotti and Doglioni, 2000), which causes along-dip variations in the vertical load and thus influences the position of ε_{xs} and, possibly, causes the widening of the area where the strike-slip configuration occurs. Eventually, strike-slip and compressive stress configurations can occur in layers with different mechanical properties but located at the same place (i.e. X and Z coordinates). An example of this lithologically-controlled switch between

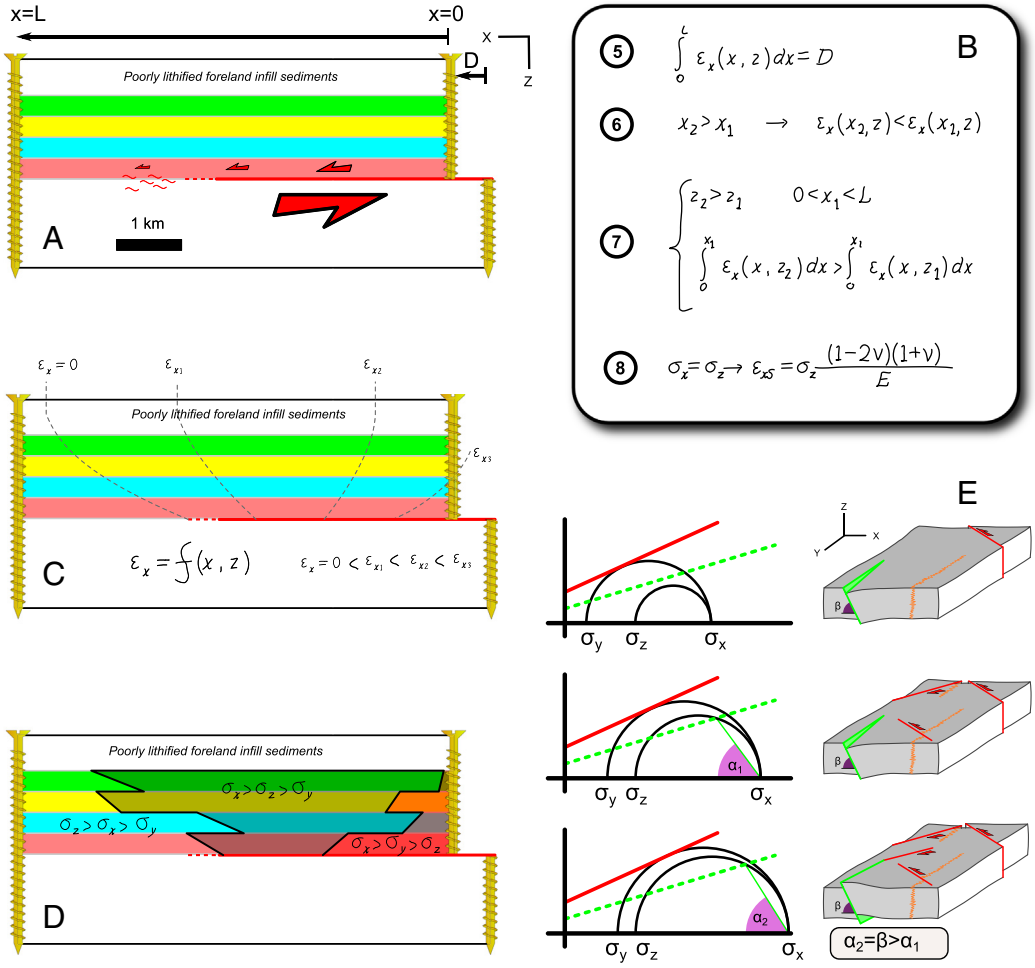

Fig. 17. Cross-sectional configuration of stress and strain during the layer parallel shortening stage. A) Geometry of the hanging wall and coordinates system. B) Equations relating X-oriented strain (ε_x) to X and Z coordinates. Equation 5 results from the observation that the sum of X-directed strains must equal the total displacement (D). Equation 6 results from the observation that the amount of strain decreases away from the site where shortening is applied. Equation 7 results from the observation that, for a fixed X-coordinate, the sum of strain must increase downward to prevent hinterlandward shear. Equation 8 provides the value of strain (named ε_{xs}) at which σ_x equals σ_z. Strain (C) and stress (D) distribution consistent with equations from 5 to 7. E) Reverse reactivation of an inherited longitudinal fault in a strike-slip stress configuration.

strike-slip and compressive stress field configurations during LPS occurs in the Scaglia Formation of the Northern Apennines, which consists of well layered limestones and marls with interbedded chert layers. In the latter, shortening is mainly accommodated by reverse faults, whilst shortening in the carbonate beds immediately above and below is accommodated by pressure solution cleavages (Alvarez et al., 1976); which are associated with bedding-perpendicular veins. Such a framework, where the shortening direction is the same in the different beds, indicates a strike-slip stress configuration in the limestone, which caused permanent deformation preventing the transition to a compressive stress field configuration. On the other hand, a compressional stress field configuration occurred in the chert, where no permanent deformation occurred before compressive failure. At a larger scale, this scenario is consistent with the observation that reverse fault nucleation tends to occur in stiff layers (e.g. Eisenstadt and De Paor, 1987; Chester et al., 1991). There, high values of the Young modulus imply the onset of a compressive stress field whilst the stress configuration in the surrounding layers is still strike-slip (equation 8 of Fig. 17B). After thrust ramp nucleation and propagation (upward and, in some cases, downward to link with the basal decollement level; e.g. Williams and Chapman, 1983; Eisenstadt and De Paor, 1987; Ellis and Dunlap, 1988; Morley, 1994; McConnell et al., 1997; Storti et al., 1997), the increase of displacement applied to the edge of the model (i.e. D in Fig. 17A) no longer implies an increase of stress in the faulted layers because it is mostly accommodated by slip along the fault. Conversely, the unfaulted layers experience increasing strain, which is essentially the reason for the syn-folding layer-parallel shortening documented in the previous sections. It is worth noting that, as the displacement applied to the edge of the model increases, the amount of syn-folding strain in the unfaulted layers increases through time until the thrust ramp cuts through them (e.g. Tavani et al., 2006b). Such a strain increase has to occur specifically ahead of the propagating fault tip. This area is in fact the process zone of the fault, where fracturing is expected to occur in order to accommodate the relative displacement between hanging wall and footwall in the lack of a localised fault zone (e.g. Cowie and Scholz, 1992), as predicted in trishear fault propagation folding (e.g. Erslev, 1991; Allmendinger, 1998).

We have shown that a thrust ramp can nucleate in a strike-slip stress field configuration, where local compressional stress conditions may exist because of combined depth and lithological effects. This vertical transition from strike-slip to compression at depth has been documented for example in an active thrust-related anticline of the Apennines, where transition from strike-slip to extension in the uppermost levels also occurs (Carminati et al., 2010). Our observations also fit leak-off tests performed in wells of active thrust-belts, which frequently indicate that the horizontal stress can be the minimum stress component (e.g. Couzens-Schultz and Chan, 2010).

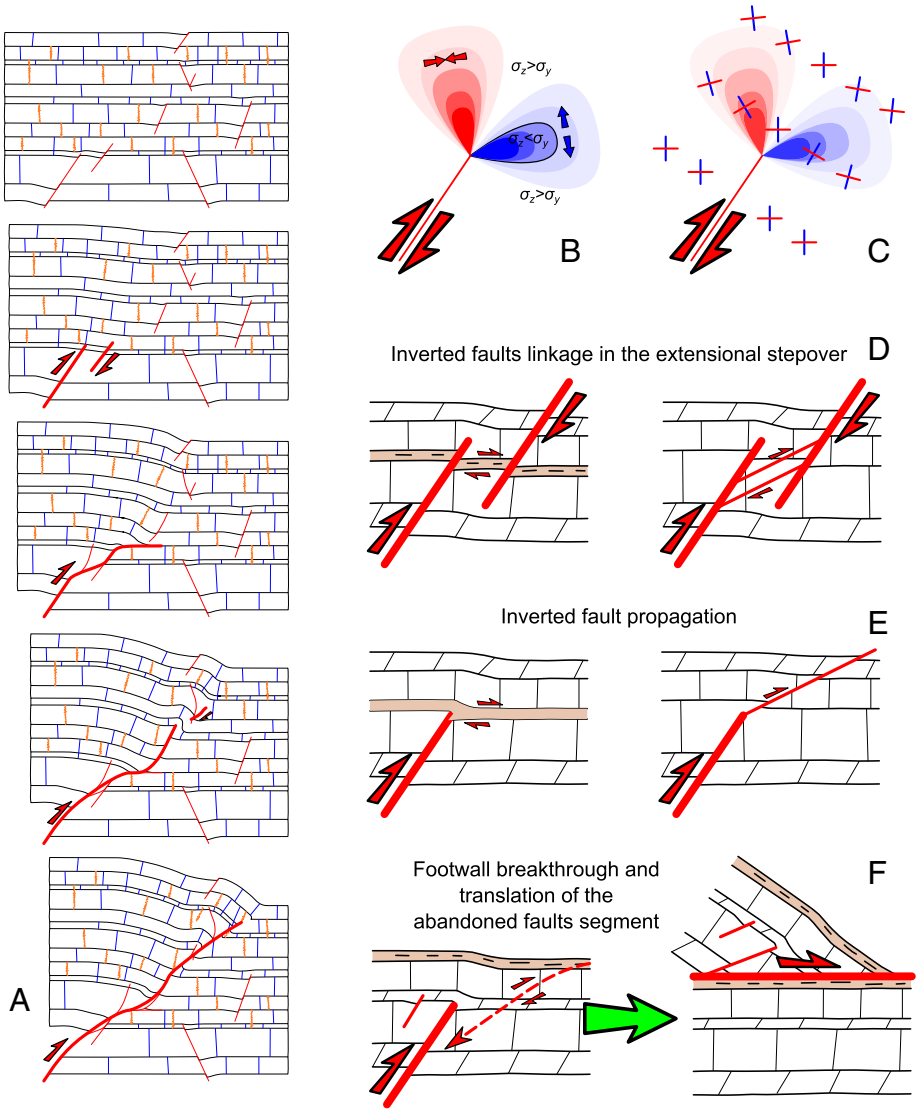

Fig. 18. A) Scheme showing thrust nucleation and propagation in a previously fractured rock volume. Stress perturbation at the fault tip, with extensional and compressional quadrants (B) and trajectories of the regional maximum and intermediate stress axes (C) indicated. D) Linkage of inverted faults throughout a layer-parallel decollement or a newly formed faults in the extensional stepover. E) Upward propagation of an inverted fault along a layer parallel decollement or a newly formed reverse fault. F) Breakthrough in the foot-wall of a positively inverted fault, with geometry after hanging wall translation above an upper decollement.

When the role of inherited deformation structures is taken into account, a compressive stress configuration may be not required for triggering thrusting, as supported by previously described field examples showing that inversion tectonics mostly occurs with weak contractional/strike slip deformation. Generally, stress and fluid conditions may favour the reactivation of inherited low-cohesion and low-friction faults instead of the development of new ones (e.g. Sibson, 1985, 1995). This process includes the possibility of reactivating surfaces that do not contain the intermediate principal stress axis (e.g. Blenkinsop, 2008). This is illustrated in Fig. 17E, where it is shown that, in a strike-slip stress field configuration, progressive stress build up can lead to the reactivation of an inherited normal fault containing the minimum principal stress axis (σ_3). Accordingly, and due to the positive influence exerted by inherited and precursory fractures in favouring the nucleation and propagation of faults (e.g. Kim et al., 2003; Crider and Peacock, 2004; Shiner et al., 2004; Healy et al., 2006; Nenna and Aydin, 2011), the occurrence of longitudinal inheritance can favour thrust fault nucleation (Fig. 18A). Strain oriented parallel to the slip direction, which occurs at the tip of positively inverted faults or in the overstep area between them, produces local perturbations of the stress field (e.g. Pollard and Segall, 1987). This causes: (i) the development of dilational and contractional areas emanating from the tip of the fault (Fig. 18B), and (ii) the rotation of the maximum stress axis that can attain a favourable angle with respect to layers, allowing slip along bedding surfaces (Fig. 18C). In the case of fault inversion within the framework of a strike-slip stress field configuration, process (i) can cause the local permutation between minimum and intermediate principal axes of the stress ellipsoid in the dilational areas, favouring the onset of a compressional stress field around the fault tip and, consequently, the propagation of the fault through an about 30° dipping, newly formed segment. On the other hand, positive inversion of widespread inherited deformation structures can occur in a strike-slip stress field configuration by process (ii). Linkage (Fig. 18D) and/or propagation (Fig. 18E) of positively inverted faults may be provided either by low-friction bedding surfaces or newly formed fault strands which develop due to the establishment of a local compressional stress field configuration. It is worth noting that, after folding of the strata ahead of the upward propagating thrust ramp begins, and depending on the amount of tilting, any kind of longitudinal structure (i.e. faults, joints, pressure solution cleavage) can attain a favourable orientation for shear re-activation. Essentially, progressive folding further facilitates ramp propagation by linkage of a progressively better

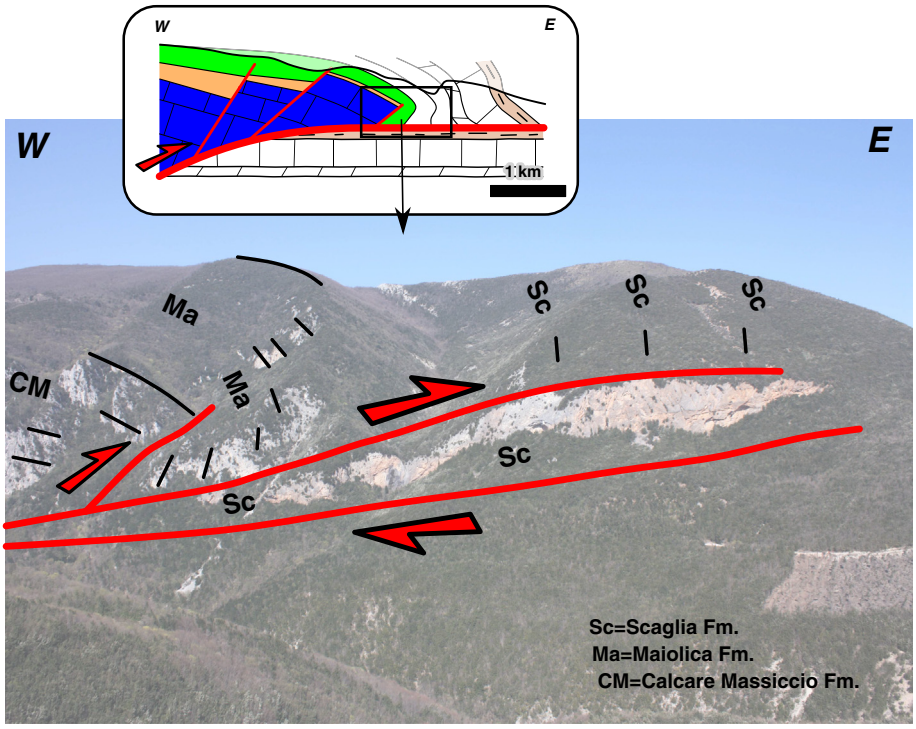

Fig. 19. Cross-section and panoramic photo along the Sibillini Thrust of the Northern Apennines, with fossil forced folds associated with the translation of an inverted and then abandoned inherited extensional fault.

oriented dense network of deformation structures. Development of a thrust requires that many inherited extensional faults are totally or partially inverted, the latter being possibly preserved in the folded hanging wall (Fig. 18F). This is the case of the southern portion of the Northern Apennines (Fig. 19), where N–S striking Jurassic extensional faults are exposed in the hanging wall of N–S striking Miocene to Pliocene thrust-related anticlines (e.g. Pierantoni et al., 2013), and transported forced folds record the early inversion of these faults, which has occurred in a strike-slip stress field configuration (Tavani et al., 2012a).

To summarize, thrust nucleation and propagation can be facilitated by the occurrence and reactivation of inherited pre- and/or early-orogenic deformation structures, whose reactivation prevents large stress accumulation in the thrust sheets before and during thrusting and folding. The positive inversion of these inherited deformation patterns, in fact, may occur in a strike slip stress field configuration as it requires stress magnitudes lower than those necessary to develop a new thrust. In this case, the hanging wall is dominated by pre-folding structural assemblages, which may undergo reactivation and modification of the original crosscutting and abutting relationships during LPS and folding stages. Conversely, when pre- and/or early-orogenic structures are not widespread or are not systematically reactivated, larger stress accumulations are required to form thrust faults, so that the stress field can easily reach a compressive configuration and, contextually, LPS and syn-folding patterns are expected to develop in the poorly fractured multilayer.

4. Conclusions

We have shown that deformation patterns characterising foreland thrust and fold belts indicate that thrusting occurs both in strike-slip and reverse faulting stress field configurations, i.e. with a near vertical attitude of the intermediate and minimum principal axis of the stress ellipsoid, respectively. To address the problem of how thrusts can nucleate in a strike-slip stress field configuration, we emphasize the fundamental role played by pre- and early-orogenic structural inheritance on the nucleation and propagation of thrust surfaces. Pre-existing longitudinal deformation structures can lead to the development of large thrusts and reverse faults even in a fully strike-slip stress field configuration. Depth and rheology can favour local compressional stress configuration in the fault process zone, facilitating fault tip migration. During the long-lasting deformation history of particles migrating from the foreland into the thrust-and-fold belt, different deformation stages triggered by different stress field configurations occur and imply repeated stress-switching events between the principal axes of the stress ellipsoid, which are fundamentally influenced by structural inheritance. Since the transmission of orogenic stress and stress build-up through the cover and the faulted basement of forelands is likely heterogeneous and complex, the role of deformation structures unrelated to cover folding but linked to far-field orogenic stresses and foreland flexure has to be carefully considered to build more realistic conceptual models of folding-related fracture pattern evolution. Shearing and reopening of pre-existing vein/fracture sets appear to be a very important mechanism to control the brittle deformation pattern within fault-related cover folds.

Acknowledgments

The contents of this paper benefit from long-lasting working activity in many thrust-fold belts worldwide, supported by both public and industrial funding. Discussions with many colleagues contributed to better focus the contents of this review. We are greatly indebted with the reviewers Chris Morley, Richard Lisle and François Roure for their very constructive comments and suggestions that helped us to significantly improve the manuscript. We acknowledge the editorial advice of Carlo Doglioni.

References

Ahmadhadi, F., Lacombe, O., Daniel, J.M., 2007. Early reactivation of basement faults in Central Zagros (SW Iran): evidence from pre-folding fracture populations in Asmari Formation and lower Tertiary paleogeography. Thrust Belts and Foreland Basins. Springer, Berlin Heidelberg, pp. 205–228.

Ahmadhadi, F., Daniel, J.M., Azzizadeh, M., Lacombe, O., 2008. Evidence for pre-folding vein development in the Oligo-Miocene Asmari Formation in the Central Zagros Fold Belt, Iran. Tectonics 27 (1), TC1016.

Allmendinger, R.W., 1982. Analysis of microstructures in the Meade plate of the Idaho–Wyoming foreland thrust belt, USA. Tectonophysics 85 (3), 221–251.

Allmendinger, R.W., 1998. Inverse and forward numerical modeling of trishear fault-propagation folds. Tectonics 17 (4), 640–656.

Alvarez, W., Engelder, T., Lowrie, W., 1976. Formation of spaced cleavage and folds in brittle limestone by dissolution. Geology 4 (11), 698–701.

Alvarez, W., Engelder, T., Geiser, P.A., 1978. Classification of solution cleavage in pelagic limestones. Geology 6 (5), 263–266.

Amrouch, K., Lacombe, O., Bellahsen, N., Daniel, J.M., Callot, J.P., 2010a. Stress and strain patterns, kinematics and deformation mechanisms in a basement-cored anticline: Sheep Mountain Anticline, Wyoming. Tectonics 29 (1), TC1005. http://dx.doi.org/10.1029/2009TC002525.

Amrouch, K., Robion, P., Callot, J.P., Lacombe, O., Daniel, J.M., Bellahsen, N., Faure, J.L., 2010b. Constraints on deformation mechanisms during folding provided by rock physical properties: a case study at Sheep Mountain anticline (Wyoming, USA). Geophys. J. Int. 182 (3), 1105–1123.

Amrouch, K., Beaudoin, N., Lacombe, O., Bellahsen, N., Daniel, J.M., 2011. Paleostress magnitudes in folded sedimentary rocks. Geophys. Res. Lett. 38 (17), L17301.

Anastasio, D.J., Fisher, D.M., Messina, T.A., Holl, J.E., 1997. Kinematics of décollement folding in the Lost River Range, Idaho. J. Struct. Geol. 19 (3), 355–368.

Anderson, E.M., 1951. The Dynamics of Faulting. Oliver and Boyd, Edinburgh.

Aubourg, C., Smith, B., Eshrahi, A., Lacombe, O., Authemayou, C., Amrouch, K., Bellier, O., Mouthereau, F., 2010. New magnetic fabric data and their comparison with stress/strain markers from the Western Fars arc (Zagros); tectonic implications. Geol. Soc. Lond., Spec. Publ. 330, 97–120.

Averbuch, O., Frizon de Lamotte, D., Kissel, C., 1992. Magnetic fabric as a structural indicator of the deformation path within a fold-thrust structure: a test case from the Corbières (NE Pyrenees, France). J. Struct. Geol. 14 (4), 461–474.

Awdal, A.H., Braathen, A., Wennberg, O.P., Sherwani, G.H., 2013. The characteristics of fracture networks in the Shiranish Formation of the Bina Bawi Anticline; comparison with the Taq Taq Field, Zagros, Kurdistan, NE Iraq. Pet. Geosci. 19 (2), 139–155.

Bai, T., Maerten, L., Gross, M.R., Aydin, A., 2002. Orthogonal cross joints: do they imply a regional stress rotation? J. Struct. Geol. 24 (1), 77–88.

Bazalgette, L., Petit, J.P., Amrhar, M., Ouanaïmi, H., 2010. Aspects and origins of fractured dip-domain boundaries in folded carbonate rocks. J. Struct. Geol. 32 (4), 523–536.

Beaudoin, N., Leprêtre, R., Bellahsen, N., Lacombe, O., Amrouch, K., Callot, J.P., Emmanuel, L., Daniel, J.M., 2012. Structural and microstructural evolution of the Rattlesnake Mountain Anticline (Wyoming, USA): new insights into the Sevier and Laramide orogenic stress build-up in the Bighorn Basin. Tectonophysics 576, 20–45.

Beaumont, C., Ellis, S., Hamilton, J., Fullsack, P., 1996. Mechanical model for subduction–collision tectonics of Alpine-type compressional orogens. Geology 24 (8), 675–678.

Bellahsen, N., Fiore, P., Pollard, D.D., 2006a. The role of fractures in the structural interpretation of Sheep Mountain Anticline, Wyoming. J. Struct. Geol. 28 (5), 850–867.

Bellahsen, N., Fiore, P.E., Pollard, D.D., 2006b. From spatial variation of fracture patterns to fold kinematics: a geomechanical approach. Geophys. Res. Lett. 33 (2), L02301.

Bergbauer, S., Pollard, D.D., 2004. A new conceptual fold-fracture model including prefolding joints, based on the Emigrant Gap anticline, Wyoming. Geol. Soc. Am. Bull. 116, 294–307.

Billi, A., Salvini, F., 2003. Development of systematic joints in response to flexure-related fibre stress in flexed foreland plates: the Apulian forebulge case history, Italy. J. Geodyn. 36 (4), 523–536.

Blenkinsop, T.G., 2008. Relationships between faults, extension fractures and veins, and stress. J. Struct. Geol. 30 (5), 622–632.

Bobillo-Ares, N.C., Bastida, F., Aller, J., 2000. On tangential longitudinal strain folding. Tectonophysics 319 (1), 53–68.

Bradley, D.C., Kidd, W.S.F., 1991. Flexural extension of the upper continental crust in collisional foredeeps. Geol. Soc. Am. Bull. 103 (11), 1416–1438.

Calamita, F., Deiana, G., 1980. Evidenze di una fase tettonica distensiva del Messiniano basale nel bacino di Camerino (Appennino umbro-marchigiano). Studi Geol. Camerti 7, 7–11.

Cardozo, N., Jackson, C.A.L., Whipp, P.S., 2011. Determining the uniqueness of best-fit trishear models. J. Struct. Geol. 33 (6), 1063–1078.

Carminati, E., Scrocca, D., Doglioni, C., 2010. Compaction-induced stress variations with depth in an active anticline: Northern Apennines, Italy. J. Geophys. Res. Solid Earth 115, B02401. http://dx.doi.org/10.1029/2009JB006395.

Carminati, E., Aldega, L., Bigi, S., Corrado, S., D'Ambrogi, C., Mohammadi, P., Shaban, A., Sherkati, S., 2013. Control of Cambrian evaporites on fracturing in fault-related anticlines in the Zagros fold-and-thrust belt. Int. J. Earth Sci. 102, 1237–1255. http://dx.doi.org/10.1007/s00531-012-0858-0.

Casini, G., Gillespie, P.A., Vergés, J., Romaire, I., Fernández, N., Casciello, E., Hunt, D.W., 2011. Sub-seismic fractures in foreland fold and thrust belts: insight from the Lurestan Province, Zagros Mountains, Iran. Pet. Geosci. 17 (3), 263–282.

Célérier, B., Etchecopar, A., Bergerat, F., Vergely, P., Artaud, F., Laurent, P., 2012. Inferring stress from faulting: from early concepts to inverse methods. Tectonophysics 581, 206–219.

Chapman, T.J., Williams, G.D., 1984. Displacement–distance methods in the analysis of fold-thrust structures and linked-fault systems. J. Geol. Soc. 141 (1), 121–128.

Chapple, W.M., 1978. Mechanics of thin-skinned fold-and-thrust belts. Geol. Soc. Am. Bull. 89 (8), 1189–1198.

Chapple, W.M., Spang, J.H., 1974. Significance of layer-parallel slip during folding of layered sedimentary rocks. Geol. Soc. Am. Bull. 85 (10), 1523–1534.

Chester, J.S., Chester, F.M., 1990. Fault-propagation folds above thrusts with constant dip. J. Struct. Geol. 12 (7), 903–910.

Chester, J.S., Logan, J.M., Spang, J.H., 1991. Influence of layering and boundary conditions on fault-bend and fault-propagation folding. Geol. Soc. Am. Bull. 103 (8), 1059–1072.

Chu, H.T., Lee, J.C., Bergerat, F., Hu, J.C., Liang, S.H., Lu, C.Y., Lee, T.Q., 2013. Fracture patterns and their relations to mountain building in a fold-thrust belt: a case study in NW Taiwan. Bull. Soc. Geol. Fr. 184 (4–5), 485–500.

Conrad, C.P., Lithgow-Bertelloni, C., 2002. How mantle slabs drive plate tectonics. Science 298, 207–209.

Cooper, M., 1992. The analysis of fracture systems in subsurface thrust structures from the Foothills of the Canadian Rockies. Thrust tectonics 391–405.

Cooper, M.A., Garton, M.R., Hossack, J.R., 1983. The origin of the Basse Normandie duplex, Boulonnais, France. J. Struct. Geol. 5 (2), 139–152.

Couzens-Schultz, B.A., Chan, A.W., 2010. Stress determination in active thrust belts: an alternative leak-off pressure interpretation. J. Struct. Geol. 32 (8), 1061–1069.

Coward, M.P., Enfield, M.A., Fischer, M.W., 1989. Devonian basins of Northern Scotland: extension and inversion related to Late Caledonian–Variscan tectonics. Geol. Soc. Lond., Spec. Publ. 44 (1), 275–308.

Cowie, P.A., Scholz, C.H., 1992. Displacement–length scaling relationship for faults: data synthesis and discussion. J. Struct. Geol. 14 (10), 1149–1156.

Crider, J.G., Peacock, D.C., 2004. Initiation of brittle faults in the upper crust: a review of field observations. J. Struct. Geol. 26 (4), 691–707.

Crosby, G.W., 1969. Radial movements in the western Wyoming salient of the Cordilleran overthrust belt. Geol. Soc. Am. Bull. 80 (6), 1061–1078.

Dahlen, F.A., Suppe, J., Davis, D., 1984. Mechanics of fold-and-thrust belts and accretionary wedges: cohesive Coulomb theory. J. Geophys. Res. Solid Earth 89 (B12), 10087–10101.

Dahlstrom, C.D.A., 1969. Balanced cross sections. Can. J. Earth Sci. 6 (4), 743–757.

Dart, C.J., McClay, K., Hollings, P.N., 1995. 3D analysis of inverted extensional fault systems, southern Bristol Channel basin, UK. Geol. Soc. Lond., Spec. Publ. 88 (1), 393–413.

Davis, D., Suppe, J., Dahlen, F.A., 1983. Mechanics of fold-and-thrust belts and accretionary wedges. J. Geophys. Res. Solid Earth 88 (B2), 1153–1172.

De Paola, N., Mirabella, F., Barchi, M.R., Burchielli, F., 2006. Early orogenic normal faults and their reactivation during thrust belt evolution: the Gubbio Fault case study, Umbria-Marche Apennines (Italy). J. Struct. Geol. 28 (11), 1948–1957.

De Paor, D.G., Simpson, C., Bailey, C.M., McCaffrey, K.J., Beam, E., Gower, R.J., Aziz, G., 1991. The role of solution in the formation of boudinage and transverse veins in carbonate rocks at Rheems, Pennsylvania. Geol. Soc. Am. Bull. 103 (12), 1552–1563.

De Sitter, L.U., 1956. Structural Geology. McGraw-Hill, New York.

DeCelles, P.G., Giles, K.A., 1996. Foreland basin systems. Basin Res. 8 (2), 105–123.

Destro, N., 1995. Release fault: a variety of cross fault in linked extensional fault systems, in the Sergipe–Alagoas Basin, NE Brazil. J. Struct. Geol. 17 (5), 615–629.

Dietrich, D., 1989. Fold-axis parallel extension in an arcuate fold-and thrust belt: the case of the Helvetic nappes. Tectonophysics 170 (3), 183–212.

Doglioni, C., 1995. Geological remarks on the relationships between extension and convergent geodynamic settings. Tectonophysics 252 (1), 253–267.

Doglioni, C., Prosser, G., 1997. Fold uplift versus regional subsidence and sedimentation rate. Mar. Pet. Geol. 14 (2), 179–190.

Doglioni, C., Merlini, S., Cantarella, G., 1999. Foredeep geometries at the front of the Apennines in the Ionian sea (central Mediterranean). Earth Planet. Sci. Lett. 168 (3–4), 243–254.

Donath, F.A., Parker, R.B., 1964. Folds and folding. Geol. Soc. Am. Bull. 75 (1), 45–62.

Eisenstadt, G., De Paor, D.G., 1987. Alternative model of thrust–fault propagation. Geology 15 (7), 630–633.

Elliott, D., 1976. The motion of thrust sheets. J. Geophys. Res. 81 (5), 949–963.

Ellis, M.A., Dunlap, W.J., 1988. Displacement variation along thrust faults: Implications for the development of large faults. J. Struct. Geol. 10 (2), 183–192.

Engelder, T., Engelder, R., 1977. Fossil distortion and decollement tectonics of the Appalachian Plateau. Geology 5 (8), 457–460.

Engelder, T., Geiser, P., 1980. On the use of regional joint sets as trajectories of paleostress fields during the development of the Appalachian Plateau, New York. J. Geophys. Res. 85 (B11), 6319–6341.

Engelder, T., Marshak, S., 1985. Disjunctive cleavage formed at shallow depths in sedimentary rocks. J. Struct. Geol. 7 (3), 327–343.

Erslev, E.A., 1991. Trishear fault-propagation folding. Geology 19 (6), 617–620.

Erslev, E.A., 2001. Multistage, multidirectional Tertiary shortening and compression in north-central New Mexico. Geol. Soc. Am. Bull. 113 (1), 63–74.

Erslev, E.A., Koenig, N.V., 2009. Three-dimensional kinematics of Laramide, basement-involved Rocky Mountain deformation, USA: insights from minor faults and GIS-enhanced structure maps. In: Kay, S.M., Ramos, V.A., Dickinson, W.R. (Eds.), Backbone of the Americas: Shallow Subduction, Plateau Uplift, and Ridge and Terrane Collision. Geological Society of America Memoir 204, pp. 125–150.

Erslev, E.A., Mayborn, K.R., 1997. Multiple geometries and modes of fault-propagation folding in the Canadian thrust belt. J. Struct. Geol. 19 (3), 321–335.

Erslev, E.A., Rogers, J.L., 1993. Basement-cover geometry of Laramide fault-propagation folds. Geol. Soc. Am. Spec. Pap. 280, 125–146.

Evans, M.A., 2010. Temporal and spatial changes in deformation conditions during the formation of the Central Appalachian fold-and-thrust belt: Evidence from joints, vein mineral paragenesis, and fluid inclusions. From Rodinia to Pangea: The Lithotectonic Record of the Appalachian Region 206, p. 477.

Evans, M.A., Dunne, W.M., 1991. Strain factorization and partitioning in the North Mountain thrust sheet, central Appalachians, USA. J. Struct. Geol. 13 (1), 21–35.

Evans, M.A., Elmore, R.D., 2006. Fluid control of localized mineral domains in limestone pressure solution structures. J. Struct. Geol. 28 (2), 284–301.

Evans, M.A., Lewchuk, M.T., Elmore, R.D., 2003. Strain partitioning of deformation mechanisms in limestones: examining the relationship of strain and anisotropy of magnetic susceptibility (AMS). J. Struct. Geol. 25 (9), 1525–1549.

Faill, R.T., 1973. Kink-band folding, Valley and Ridge province, Pennsylvania. Geol. Soc. Am. Bull. 84 (4), 1289–1314.
Ferrill, D.A., Dunne, W.M., 1989. Cover deformation above a blind duplex: an example from West Virginia, USA. J. Struct. Geol. 11 (4), 421–431.
Ferrill, D.A., Groshong, R.H., 1993. Kinematic model for the curvature of the northern Subalpine Chain, France. J. Struct. Geol. 15 (3), 523–541.
Fischer, M.P., Christensen, R.D., 2004. Insights into the growth of basement uplifts deduced from a study of fracture systems in the San Rafael monocline, east central Utah. Tectonics 23 (1).
Fischer, M.P., Jackson, P.B., 1999. Stratigraphic controls on deformation patterns in fault-related folds: a detachment fold example from the Sierra Madre Oriental, northeast Mexico. J. Struct. Geol. 21 (6), 613–633.
Fischer, M.P., Wilkerson, M.S., 2000. Predicting the orientation of joints from fold shape: results of pseudo-three-dimensional modeling and curvature analysis. Geology 28 (1), 15–18.
Fletcher, R.C., 1989. Approximate analytical solutions for a cohesive fold-and-thrust wedge: some results for lateral variation in wedge properties and for finite wedge angle. J. Geophys. Res. Solid Earth 94 (B8), 10347–10354.
Fletcher, R.C., Pollard, D.D., 1981. Anticrack model for pressure solution surfaces. Geology 9 (9), 419–424.
Frehner, M., 2011. The neutral lines in buckle folds. J. Struct. Geol. 33 (10), 1501–1508.
Geiser, P.A., 1988. Mechanisms of thrust propagation: some examples and implications for the analysis of overthrust terranes. J. Struct. Geol. 10 (8), 829–845.
Geiser, P., Engelder, T., 1983. The distribution of layer parallel shortening fabrics in the Appalachian foreland of New York and Pennsylvania: evidence for two non-coaxial phases of the Alleghanian orogeny. Contributions to the Tectonics and Geophysics of Mountain Chains: Geological Society of America Memoir 158, pp. 161–175.
Geiser, P.A., Sansone, S., 1981. Joints, microfractures, and the formation of solution cleavage in limestone. Geology 9 (6), 280–285.
Glen, R.A., Hancock, P.L., Whittaker, A., 2005. Basin inversion by distributed deformation: the southern margin of the Bristol Channel Basin, England. J. Struct. Geol. 27 (12), 2113–2134.
Gonzales, J., Aydin, A., 2008. Structural characterization of deep-water deposits in a foreland basin, Silla Syncline (Chilean Patagonia), with applications to depositional processes. J. Struct. Geol. 30 (9), 1095–1108.
Graham, B., Antonellini, M., Aydin, A., 2003. Formation and growth of normal faults in carbonates within a compressive environment. Geology 31 (1), 11–14.
Gray, M.B., Mitra, G., 1993. Migration of deformation fronts during progressive deformation: evidence from detailed structural studies in the Pennsylvania Anthracite region, USA. J. Struct. Geol. 15 (3), 435–449.
Gross, M.R., 1993. The origin and spacing of cross joints: examples from the Monterey Formation, Santa Barbara Coastline, California. J. Struct. Geol. 15 (6), 737–751.
Guillaume, B., Dhont, D., Brusset, S., 2008. Three-dimensional geologic imaging and tectonic control on stratigraphic architecture: upper cretaceous of the Tremp Basin (south-central Pyrenees, Spain). Am. Assoc. Pet. Geol. Bull. 92 (2), 249–269.
Guiton, M.L.E., Sassi, W., Leroy, Y.M., Gauthier, B.D.M., 2003a. Mechanical constraints on the chronology of fracture activation in folded Devonian sandstone of the western Moroccan Anti-Atlas. J. Struct. Geol. 25, 1317–1330.
Guiton, M.L.E., Leroy, Y.M., Sassi, W., 2003b. Activation of diffuse discontinuities and folding of sedimentary layers. J. Geophys. Res. Solid Earth 108 (2183), C4. http://dx.doi.org/10.1029/2002JB001770.
Gutiérrez-Alonso, G., Gross, M.R., 1999. Structures and mechanisms associated with development of a fold in the Cantabrian Zone thrust belt, NW Spain. J. Struct. Geol. 21 (6), 653–670.
Hancock, P.L., 1985. Brittle microtectonics: principles and practice. J. Struct. Geol. 7 (3), 437–457.
Hardy, S., Ford, M., 1997. Numerical modeling of trishear fault propagation folding. Tectonics 16 (5), 841–854.
Healy, D., Jones, R.R., Holdsworth, R.E., 2006. Three-dimensional brittle shear fracturing by tensile crack interaction. Nature 439, 64–67.
Hessami, K., Koyi, H.A., Talbot, C., 2001. The significance of strike-slip faulting in the basement of the Zagros fold-and-thrust belt. J. Pet. Geol. 24 (1–4), 5–28.
Holl, J.E., Anastasio, D.J., 1995. Cleavage development within a foreland fold and thrust belt, southern Pyrenees, Spain. J. Struct. Geol. 17 (3), 357–369.
Homberg, C., Lacombe, O., Angelier, J., Bergerat, F., 1999. New constraints for indentation mechanisms from the Jura Mountains (France). Geology 27 (9), 827–830.
Homberg, C., Bergerat, F., Philippe, Y., Lacombe, O., Angelier, J., 2002. Structural inheritance and Cenozoic stress fields in the Jura fold-and-thrust belt. Tectonophysics 357, 137–158.
Hudleston, P.J., Holst, T.B., 1984. Strain analysis and fold shape in a limestone layer and implications for layer rheology. Tectonophysics 106 (3), 321–347.
Hudleston, P.J., Treagus, S.H., 2010. Information from folds: a review. J. Struct. Geol. 32 (12), 2042–2071.
Ismat, Z., 2008. Folding kinematics expressed in fracture patterns: an example from the Anti-Atlas fold belt, Morocco. J. Struct. Geol. 30 (11), 1396–1404.
Jamison, W.R., 1987. Geometric analysis of fold development in overthrust terranes. J. Struct. Geol. 9 (2), 207–219.
Keating, D.P., Fischer, M.P., Blau, H., 2012. Physical modeling of deformation patterns in monoclines above oblique-slip faults. J. Struct. Geol. 39, 37–51.
Kelly, P.G., Peacock, D.C.P., Sanderson, D.J., McGurk, A.C., 1999. Selective reverse-reactivation of normal faults, and deformation around reverse-reactivated faults in the Mesozoic of the Somerset coast. J. Struct. Geol. 21 (5), 493–509.
Kim, Y.S., Peacock, D.C.P., Sanderson, D.J., 2003. Mesoscale strike-slip faults and damage zones at Marsalforn, Gozo Island, Malta. J. Struct. Geol. 25 (5), 793–812.
Koons, P.O., 1995. Modeling the topographic evolution of collisional belts. Annu. Rev. Earth Planet. Sci. 23 (1), 375–408.
Koyi, H.A., Sans, M., Teixell, A., Cotton, J., Zeyen, H., 2004. The significance of penetrative strain in the restoration of shortened layers—insights from sand models and the Spanish Pyrenees. *Thrust, tectonics and hydrocarbon systems*. AAPG Mem. 82, 207–222.
Lacombe, O., 2010. Calcite twins, a tool for tectonic studies in thrust belts and stable orogenic forelands. Oil and Gas Science and Technology 65 (6), 809–838.
Lacombe, O., 2012. Do fault slip data inversions actually yield 'paleostresses' that can be compared with contemporary stresses? A critical discussion. Compt. Rendus Geosci. 344, 159–173.
Lacombe, O., Mouthereau, F., 1999. What is the real front of orogens? The Pyrenean orogen case. C. R. Acad. Sci. 329 (II), 889–896.
Lacombe, O., Mouthereau, F., Deffontaines, B., Angelier, J., Chu, H.-T., Lee, C.T., 1999. Geometry and quaternary kinematics of fold-and-thrust units of SW Taiwan. Tectonics 18 (6), 1198–1223.
Lacombe, O., Mouthereau, F., Angelier, J., Chu, H.T., Lee, J.C., 2003. Frontal belt curvature and oblique ramp development at an obliquely collided irregular margin: geometry and kinematics of the NW Taiwan fold–thrust belt. Tectonics 22 (3), 1025.
Lacombe, O., Mouthereau, F., Kargar, S., Meyer, B., 2006. Late Cenozoic and modern stress fields in the western Fars (Iran): implications for the tectonic and kinematic evolution of central Zagros. Tectonics 25 (1), TC1003.
Lacombe, O., Amrouch, K., Mouthereau, F., Dissez, L., 2007. Calcite twinning constraints on late Neogene stress patterns and deformation mechanisms in the active Zagros collision belt. Geology 35 (3), 263–266.
Lacombe, O., Bellahsen, N., Mouthereau, F., 2011. Fracture patterns in the Zagros Simply Folded Belt (Fars, Iran): constraints on early collisional tectonic history and role of basement faults. Geol. Mag. 148 (5–6), 940–963.
Lacombe, O., Tavani, S., Soto, R., 2012. An introduction to the Tectonophysics special issue "Into the deformation history of folded rocks". Tectonophysics 576–577, 1–3.
Laird, A.P., Morley, C.K., 2011. Development of gas hydrates in a deep-water anticline based on attribute analysis from three-dimensional seismic data. Geosphere 7 (1), 240–259.
Langhi, L., Ciftci, N.B., Borel, G.D., 2011. Impact of lithospheric flexure on the evolution of shallow faults in the Timor foreland system. Mar. Geol. 284 (1), 40–54.
Lash, G.G., Engelder, T., 2007. Jointing within the outer arc of a forebulge at the onset of the Alleghanian Orogeny. J. Struct. Geol. 29 (5), 774–786.
Lemiszki, P.J., Landes, J.D., Hatcher, R.D., 1994. Controls on hinge-parallel extension fracturing in single-layer tangential-longitudinal strain folds. J. Geophys. Res. Solid Earth 99 (B11), 22027–22041.
Lisle, R.J., 1994. Detection of zones of abnormal strains in structures using Gaussian curvature analysis. AAPG Bull. 78 (12), 1811–1819.
Lisle, R.J., Orife, T.O., Arlegui, L., Liesa, C., Srivastava, D.C., 2006. Favoured states of palaeostress in the earth's crust: evidence from fault–slip data. J. Struct. Geol. 28 (6), 1051–1066.
Long, S., McQuarrie, N., Tobgay, T., Hawthorne, J., 2011. Quantifying internal strain and deformation temperature in the eastern Himalaya, Bhutan: implications for the evolution of strain in thrust sheets. J. Struct. Geol. 33 (4), 579–608.
Lorenzo, J.M., O'Brien, G.W., Stewart, J., Tandon, K., 1998. Inelastic yielding and forebulge shape across a modern foreland basin: North West Shelf of Australia, Timor Sea. Geophys. Res. Lett. 25 (9), 1455–1458.
Maerten, L., Maerten, F., 2006. Chronologic modeling of faulted and fractured reservoirs using geomechanically based restoration: technique and industry applications. AAPG Bull. 90 (8), 1201–1226.
Maillot, B., Koyi, H., 2006. Thrust dip and thrust refraction in fault–bend folds: analogue models and theoretical predictions. J. Struct. Geol. 28 (1), 36–49.
Mandl, G., 2000. Faulting in Brittle Rocks, An Introduction to the Mechanics of Tectonic Faults. Springer, Berlin.
Mariotti, G., Doglioni, C., 2000. The dip of the foreland monocline in the Alps and Apennines. Earth Planet. Sci. Lett. 181, 191–202.
Marshak, S., Engelder, T., 1985. Development of cleavage in limestones of a fold–thrust belt in eastern New York. J. Struct. Geol. 7 (3), 345–359.
Marshak, S., Geiser, P.A., Alvarez, W., Engelder, T., 1982. Mesoscopic fault array of the northern Umbrian Apennine fold belt, Italy: geometry of conjugate shear by pressure–solution slip. Geol. Soc. Am. Bull. 93 (10), 1013–1022.
Mastella, L., Konon, A., 2002. Jointing in the Silesian Nappe (Outer Carpathians, Poland)—paleostress reconstruction. Geol. Carpath. 53 (5), 315–326.
Matenco, L., Bertotti, G., 2000. Tertiary tectonic evolution of the external East Carpathians (Romania). Tectonophysics 316 (3), 255–286.
Mazzoli, S., Pierantoni, P.P., Borraccini, F., Paltrinieri, W., Deiana, G., 2005. Geometry, segmentation pattern and displacement variations along a major Apennine thrust zone, central Italy. J. Struct. Geol. 27 (11), 1940–1953.
McConnell, D.A., Kattenhorn, S.A., Benner, L.M., 1997. Distribution of fault slip in outcrop-scale fault-related folds, Appalachian Mountains. J. Struct. Geol. 19 (3), 257–267.
McQuarrie, N., Davis, G.H., 2002. Crossing the several scales of strain-accomplishing mechanisms in the hinterland of the central Andean fold–thrust belt, Bolivia. J. Struct. Geol. 24 (10), 1587–1602.
McQuillan, H., 1974. Fracture patterns on Kuh-e Asmari anticline, southwest Iran. AAPG Bull. 58 (2), 236–246.
Medwedeff, D.A., Krantz, R.W., 2002. Kinematic and analog modeling of 3-D extensional ramps: observations and a new 3-D deformation model. J. Struct. Geol. 24 (4), 763–772.
Mitra, S., 1990. Fault-propagation folds: geometry, kinematic evolution, and hydrocarbon traps. AAPG Bull. 74 (6), 921–945.
Mitra, G., Adolph Yonkee, W., 1985. Relationship of spaced cleavage to folds and thrusts in the Idaho–Utah–Wyoming thrust belt. J. Struct. Geol. 7 (3), 361–373.

Mitra, S., Miller, J.F., 2013. Strain variation with progressive deformation in basement-involved trishear structures. J. Struct. Geol. 53, 70–79. http://dx.doi.org/10.1016/j.jsg.2013.05.007.
Mitra, S., Mount, V.S., 1998. Foreland basement-involved structures. AAPG Bull. 82 (1), 70–109.
Mitra, G., Yonkee, W.A., Gentry, D.J., 1984. Solution cleavage and its relationship to major structures in the Idaho–Utah–Wyoming thrust belt. Geology 12 (6), 354–358.
Mollema, P.N., Antonellini, M.A., 1996. Compaction bands: a structural analog for anti-mode I cracks in aeolian sandstone. Tectonophysics 267 (1), 209–228.
Moore, G.F., Saffer, D., Studer, M., Costa Pisani, P., 2011. Structural restoration of thrusts at the toe of the Nankai Trough accretionary prism off Shikoku Island, Japan: implications for dewatering processes. Geochem. Geophys. Geosyst. 12 (5), Q0AD12.
Morley, C.K., 1986a. The Caledonian thrust front and palinspastic restorations in the southern Norwegian Caledonides. J. Struct. Geol. 8 (7), 753–765.
Morley, C.K., 1986b. A classification of thrust fronts. AAPG Bull. 70 (1), 12–25.
Morley, C.K., 1994. Fold-generated imbricates: examples from the Caledonides of Southern Norway. J. Struct. Geol. 16 (5), 619–631.
Morley, C.K., 2007. Development of crestal normal faults associated with deepwater fold growth. J. Struct. Geol. 29, 1148–1163.
Morley, C.K., Warren, J., Tingay, M., Boonyasaknanon, P., Julapour, A., 2014. Comparison of modern fluid distribution, pressure and flow in sediments associated with anticlines growing in deepwater (Brunei) and continental environments (Iran). Mar. Pet. Geol. 51, 210–229.
Mouthereau, F., Deffontaines, B., Lacombe, O., Angelier, J., 2002. Variations along the strike of the Taiwan thrust belt: Basement control on structural style, wedge geometry and kinematics. In: Byrne, T.B., Liu, C.-S. (Eds.), Geology and Geophysics of an Arc-Continent Collision, Taiwan, Republic of China, Boulder, Colorado. Geological Society of America Special Paper 358, pp. 35–58 (chapter 3).
Neely, T.G., Erslev, E.A., 2009. The interplay of fold mechanisms and basement weaknesses at the transition between Laramide basement-involved arches, north-central Wyoming, USA. J. Struct. Geol. 31 (9), 1012–1027.
Nemčok, M., Gayer, R., Miliorizos, M., 1995. Structural analysis of the inverted Bristol Channel Basin: implications for the geometry and timing of fracture porosity. Geol. Soc. Lond. Spec. Publ. 88 (1), 355–392.
Nenna, F., Aydin, A., 2011. The formation and growth of pressure solution seams in clastic rocks: a field and analytical study. J. Struct. Geol. 33 (4), 633–643.
Nickelsen, R.P., 1966. Fossil distortion and penetrative rock deformation in the Appalachian Plateau, Pennsylvania. J. Geol. 74, 924–931.
Ohlmacher, G.C., Aydin, A., 1997. Mechanics of vein, fault and solution surface formation in the Appalachian Valley and Ridge, northeastern Tennessee, USA: implications for fault friction, state of stress and fluid pressure. J. Struct. Geol. 19 (7), 927–944.
Petracchini, L., Antonellini, M., Billi, A., Scrocca, D., 2012. Fault development through fractured pelagic carbonates of the Cingoli anticline, Italy: possible analog for subsurface fluid-conductive fractures. J. Struct. Geol. 45, 21–37.
Pierantoni, P., Deiana, G., Galdenzi, S., 2013. Stratigraphic and structural features of the Sibillini Mountains (Umbria–Marche Apennines, Italy). Ital. J. Geosci. 132 (3), 497–520.
Pollard, D.D., Segall, P., 1987. Theoretical displacements and stresses near fractures in rock: with applications to faults, joints, veins, dikes, and solution surfaces. Fract. Mech. Rock 277 (349), 277–349.
Price, N.J., Cosgrove, J.W., 1990. Analysis of Geological Structures.
Protzman, G.M., Mitra, G., 1990. Strain fabric associated with the Meade thrust sheet: implications for cross-section balancing. J. Struct. Geol. 12 (4), 403–417.
Quintà, A., Tavani, S., 2012. The foreland deformation in the south-western Basque–Cantabrian Belt (Spain). Tectonophysics 576, 4–19.
Railsback, B.L., Andrews, L.M., 1995. Tectonic stylolites in the 'undeformed' Cumberland Plateau of southern Tennessee. J. Struct. Geol. 17 (6), 911–915.
Ramsay, J.G., 1967. Folding and Fracturing of Rocks. McGraw-Hill, New York.
Ramsay, J.G., 1974. Development of chevron folds. Geol. Soc. Am. Bull. 85 (11), 1741–1754.
Ranero, C.R., Morgan, J.P., McIntosh, K., Reichert, C., 2003. Bending-related faulting and mantle serpentinization at the Middle America trench. Nature 425 (6956), 367–373. http://dx.doi.org/10.1038/nature01961.
Renard, F., Ortoleva, P., Gratier, J.P., 1997. Pressure solution in sandstones: influence of clays and dependence on temperature and stress. Tectonophysics 280 (3), 257–266.
Robion, P., Humbert, F., Colombier, J.-C., Leghay, S., De Lamotte, D.F., 2012. Relationships between pore space anisotropy and anisotropy of physical properties of siliciclastic rocks from the Corbières-Minervois fold-and-thrust-belt (north-east Pyrenees, France). Tectonophysics 576–577, 63–77.
Rocher, M., Lacombe, O., Angelier, J., Deffontaines, B., Verdier, F., 2000. Cenozoic folding and faulting in the south Aquitaine Basin (France): insights from combined structural and paleostress analyses. J. Struct. Geol. 22 (5), 627–645.
Roure, F., Swennen, R., Schneider, F., Faure, J.L., Ferket, H., Guilhaumou, N., Osadetz, K., Robion, Ph., Vandeginste, V., et al., 2005. Incidence and importance of tectonics and natural fluid migration on reservoir evolution in foreland fold-and-thrust belts. In: Brosse, E. (Ed.), Oil and Gas Science and Technology, Oil and Gas Science and Technology. Revue de l'IFP 60, pp. 67–106.
Ruh, J.B., Kaus, B.J., Burg, J.P., 2012. Numerical investigation of deformation mechanics in fold-and-thrust belts: influence of rheology of single and multiple décollements. Tectonics 31 (3), TC3005. http://dx.doi.org/10.1029/2011TC003047.
Salvini, F., Storti, F., 2001. The distribution of deformation in parallel fault-related folds with migrating axial surfaces: comparison between fault-propagation and fault-bend folding. J. Struct. Geol. 23 (1), 25–32.
Sanderson, D.J., 1982. Models of strain variation in nappes and thrust sheets: a review. Tectonophysics 88 (3), 201–233.
Sans, M., Vergés, J., Gomis, E., Parés, J.M., Schiattarella, M., Travé, A., Calvet, F., Santanach, P., Doulcet, A., 2003. Layer parallel shortening in salt-detached folds: constraint on cross-section restoration. Tectonophysics 372 (1), 85–104.
Sanz, P.F., Pollard, D.D., Allwardt, P.F., Borja, R.I., 2008. Mechanical models of fracture reactivation and slip on bedding surfaces during folding of the asymmetric anticline at Sheep Mountain, Wyoming. J. Struct. Geol. 30 (9), 1177–1191.
Sassi, W., Guiton, M.L.E., Leroy, Y.M., Daniel, J.M., Callot, J.P., 2012. Constraints on bed scale fracture chronology with a FEM mechanical model of folding: the case of Split Mountain (Utah, USA). Tectonophysics 576, 197–215.
Savage, H.M., Ryan Shackleton, J., Cooke, M.L., Riedel, J.J., 2010. Insights into fold growth using fold-related joint patterns and mechanical stratigraphy. J. Struct. Geol. 32 (10), 1466–1475.
Scisciani, V., Calamita, F., Tavarnelli, E., Rusciadelli, G., Ori, G.G., Paltrinieri, W., 2001. Foreland-dipping normal faults in the inner edges of syn-orogenic basins: a case from the Central Apennines, Italy. Tectonophysics 330 (3), 211–224.
Scisciani, V., Tavarnelli, E., Calamita, F., 2002. The interaction of extensional and contractional deformations in the outer zones of the Central Apennines, Italy. J. Struct. Geol. 24 (10), 1647–1658.
Séjourné, S., Malo, M., Savard, M.M., Kirkwood, D., 2005. Multiple origin and regional significance of bedding parallel veins in a fold and thrust belt: the example of a carbonate slice along the Appalachian structural front. Tectonophysics 407 (3), 189–209.
Shackleton, J.R., Cooke, M.L., Vergés, J., Simó, T., 2011. Temporal constraints on fracturing associated with fault-related folding at Sant Corneli anticline, Spanish Pyrenees. J. Struct. Geol. 33 (1), 5–19.
Shiner, P., Beccacini, A., Mazzoli, S., 2004. Thin-skinned versus thick-skinned structural models for Apulian carbonate reservoirs: constraints from the Val d'Agri Fields, S Apennines, Italy. Mar. Pet. Geol. 21 (7), 805–827.
Sibson, R.H., 1985. A note on fault reactivation. J. Struct. Geol. 7 (6), 751–754.
Sibson, R.H., 1995. Selective fault reactivation during basin inversion: potential for fluid redistribution through fault–valve action. Geol. Soc. Lond., Spec. Publ. 88 (1), 3–19.
Silliphant, L.J., Engelder, T., Gross, M.R., 2002. The state of stress in the limb of the Split Mountain anticline, Utah: constraints placed by transected joints. J. Struct. Geol. 24 (1), 155–172.
Simpson, G., 2011. Mechanics of non-critical fold–thrust belts based on finite element models. Tectonophysics 499 (1), 142–155. http://dx.doi.org/10.1016/j.tecto.2011.01.004.
Sperner, B., Zweigel, P., 2010. A plea for more caution in fault–slip analysis. Tectonophysics 482, 29–41.
Srivastava, D.C., Engelder, T., 1990. Crack-propagation sequence and pore-fluid conditions during fault-bend folding in the Appalachian Valley and Ridge, central Pennsylvania. Geol. Soc. Am. Bull. 102 (1), 116–128.
Stearns, D.W., 1968. Certain aspects of fracture in naturally deformed rocks. Rock Mechanics Seminar: Air Force Cambridge Research Laboratory, pp. 97–118.
Stearns, D.W., Friedman, M., 1972. Reservoirs in fractured rock. AAPG Mem. 16, 82–106.
Stephenson, B.J., Koopman, A., Hillgartner, H., McQuillan, H., Bourne, S., Noad, J.J., Rawnsley, K., 2007. Structural and stratigraphic controls on fold-related fracturing in the Zagros Mountains, Iran: implications for reservoir development. Geol. Soc. Lond., Spec. Publ. 270, 1–21.
Storti, F., Poblet, J., 1997. Growth stratal architectures associated to decollement folds and fault-propagation folds. Inferences on fold kinematics. Tectonophysics 282 (1), 353–373.
Storti, F., Salvini, F., 1996. Progressive rollover fault-propagation folding: a possible kinematic mechanism to generate regional-scale recumbent folds in shallow foreland belts. AAPG Bull. 80 (2), 174–193.
Storti, F., Salvini, F., 2001. The evolution of a model trap in the Central Apennines, Italy: fracture patterns, fault reactivation and development of cataclastic rocks in carbonates at the Narni Anticline. J. Pet. Geol. 24 (2), 171–190.
Storti, F., Salvini, F., McClay, K., 1997. Fault-related folding in sandbox analogue models of thrust wedges. J. Struct. Geol. 19 (3), 583–602.
Suppe, J., 1983. Geometry and kinematics of fault–bend folding. Am. J. Sci. 283 (7), 684–721.
Suppe, J., Medwedeff, D.A., 1984. Fault-propagation folding. Geol. Soc. Am. Abstr. Programs 16, 670.
Suppe, J., Medwedeff, D.A., 1990. Geometry and kinematics of fault-propagation folding. Eclogae Geol. Helv. 83, 409–454.
Tanner, P.W., 1989. The flexural-slip mechanism. J. Struct. Geol. 11 (6), 635–655.
Tavani, S., Muñoz, J.A., 2012. Mesozoic rifting in the Basque–Cantabrian Basin (Spain): inherited faults, transversal structures and stress perturbation. Terra Nova 24 (1), 70–76.
Tavani, S., Storti, F., Fernández, O., Muñoz, J.A., Salvini, F., 2006a. 3-D deformation pattern analysis and evolution of the Anisclo anticline, southern Pyrenees. J. Struct. Geol. 28 (4), 695–712.
Tavani, S., Storti, F., Salvini, F., 2006b. Double-edge fault-propagation folding: geometry and kinematics. J. Struct. Geol. 28 (1), 19–35.
Tavani, S., Storti, F., Salvini, F., Toscano, C., 2008. Stratigraphic versus structural control on the deformation pattern associated with the evolution of the Mt. Catria anticline, Italy. J. Struct. Geol. 30 (5), 664–681.
Tavani, S., Mencos, J., Bausà, J., Muñoz, J.A., 2011a. The fracture pattern of the Sant Corneli Bóixols oblique inversion anticline (Spanish Pyrenees). J. Struct. Geol. 33 (11), 1662–1680.
Tavani, S., Storti, F., Soleimany, B., Fallah, M., Muñoz, J.A., Gambini, R., 2011b. Geometry, kinematics and fracture pattern of the Bangestan anticline, Zagros, SW Iran. Geol. Mag. 148 (5–6), 964–979.
Tavani, S., Storti, F., Bausà, J., Muñoz, J.A., 2012a. Late thrusting extensional collapse at the mountain front of the northern Apennines (Italy). Tectonics 31 (4), TC4019.
Tavani, S., Fernandez, O., Muñoz, J.A., 2012b. Stress fluctuation during thrust-related folding: Boltaña anticline (Pyrenees, Spain). Geol. Soc. Lond., Spec. Publ. 367 (1), 131–140.

Tavani, S., Snidero, M., Muñoz, J.A., 2014. Uplift-induced residual strain release and late-thrusting extension in the Anaran mountain front anticline, Zagros (Iran). Tectonophysics 636, 257–269. http://dx.doi.org/10.1016/j.tecto.2014.08.018.

Tavani, S., López, B., Muñoz, J.A., 2015. Extensional fold-related fracturing in the Armeña rollover (Cotiella Massif, Southern Pyrenees). Ital. J. Geosci. http://dx.doi.org/10.3301/IJG.2014.17 (in press).

Tavarnelli, E., 1997. Structural evolution of a foreland fold-and-thrust belt: the Umbria–Marche Apennines, Italy. J. Struct. Geol. 19 (3), 523–534.

Tavarnelli, E., Peacock, D.C., 1999. From extension to contraction in syn-orogenic foredeep basins: the Contessa section, Umbria-Marche Apennines, Italy. Terra Nova 11 (2–3), 55–60.

Thorbjornsen, K.L., Dunne, W.M., 1997. Origin of a thrust-related fold: geometric vs kinematic tests. J. Struct. Geol. 19 (3), 303–319.

Torres Carbonell, P.J., Dimieri, L.V., Martinioni, D.R., 2013. Early foreland deformation of the Fuegian Andes (Argentina): constraints from the strain analysis of Upper Cretaceous–Danian sedimentary rocks. J. Struct. Geol. 48, 14–32. http://dx.doi.org/10.1016/j.jsg.2012.12.010.

Turcotte, D., Schubert, G., 1982. Geodynamics. Wiley, New York.

Twiss, R.J., Moores, E.M., 1992. Structural Geology. Freeman, San Francisco, CA.

Twiss, R.J., Unruh, J.R., 1998. Analysis of fault slip inversions: do they constrain stress or strain rate? J. Geophys. Res. 103 (B6), 12205–12222.

Varga, R.J., 1993. Rocky Mountain foreland uplifts: products of a rotating stress field or strain partitioning? Geology 21, 1115–1118.

Weil, A.B., Yonkee, W.A., 2012. Layer-parallel shortening across the Sevier fold-thrust belt and Laramide foreland of Wyoming: spatial and temporal evolution of a complex geodynamic system. Earth Planet. Sci. Lett. 357, 405–420.

Weil, A.B., Yonkee, W.A., Kendall, J., 2014. Towards a better understanding of the influence of basement heterogeneities and lithospheric coupling on foreland deformation: a structural and paleomagnetic study of Laramide deformation in the southern Bighorn Arch, Wyoming. Geol. Soc. Am. Bull. http://dx.doi.org/10.1130/B30872.1.

Wennberg, O.P., Svånå, T., Azizzadeh, M., Aqrawi, A.M.M., Brockbank, P., Lyslo, K.B., Ogilvie, S., 2006. Fracture intensity vs. mechanical stratigraphy in platform top carbonates: the Aquitanian of the Asmari Formation, Khaviz Anticline, Zagros, SW Iran. Pet. Geosci. 12 (3), 235–246.

Whitaker, A.E., Engelder, T., 2006. Plate-scale stress fields driving the tectonic evolution of the central Ouachita salient, Oklahoma and Arkansas. Geol. Soc. Am. Bull. 118 (5–6), 710–723.

Wickham, J., 1995. Fault displacement-gradient folds and the structure at Lost Hills, California (USA). J. Struct. Geol. 17 (9), 1293–1302.

Williams, G., Chapman, T., 1983. Strains developed in the hanging walls of thrusts due to their slip/propagation rate: a dislocation model. J. Struct. Geol. 5 (6), 563–571.

Wiltschko, D.V., Medwedeff, D.A., Millson, H.E., 1985. Distribution and mechanisms of strain within rocks on the northwest ramp of Pine Mountain block, southern Appalachian foreland: a field test of theory. Geol. Soc. Am. Bull. 96 (4), 426–435.

Zehnder, A.T., Allmendinger, R.W., 2000. Velocity field for the trishear model. J. Struct. Geol. 22 (8), 1009–1014.

Zhao, M., Jacobi, R.D., 1997. Formation of regional cross-fold joints in the northern Appalachian Plateau. J. Struct. Geol. 19 (6), 817–834.